

# Incorporating Flame Spread and Fire Growth Algorithms into a Computational Zone Model

*Daniel Gojkovic*  
*Hans Hultquist*

---

Department of Fire Safety Engineering  
Lund University, Sweden

Brandteknik  
Lunds Tekniska Högskola  
Lunds Universitet

Report 5029, Lund 1999

**Incorporating Flame Spread and Fire Growth Algorithms  
into a Computational Zone Model**

**Daniel Gojkovic  
Hans Hultquist**

**Lund 1999**

# Incorporating Flame Spread and Fire Growth Algorithms into a Computational Zone Model

Daniel Gojkovic  
Hans Hultquist

**Report 5029**  
**ISSN: 1402-3504**  
**ISRN: LUTVDG/TVBB--51X--SE**

Sidantal: 86

Keywords:  
Zone model, WPI/Fire Code, flame spread, fire growth.

## Abstract:

A flame-spread model is incorporated into a zone model, the WPI/Fire Code. The external heat flux's influence on the model is discussed and a tolerable value is calculated. The input parameters to the flame-spread algorithm are exposed to a simple sensitivity analysis. The algorithm is compared with two scenarios, Model A and Model B. Model A compares experimental data from a free burning test while Method B compares data from the Room Corner Test.

© Copyright: Brandteknik, Lunds tekniska högskola, Lunds universitet, Lund 1999

---

Brandteknik  
Lunds tekniska högskola  
Lunds universitet  
Box 118  
221 00 Lund

brand@brand.lth.se  
<http://www.brand.lth.se>

Telefon: 046 - 222 73 60  
Telefax: 046 - 222 46 12

Department of Fire Safety Engineering  
Lund University  
Box 118  
SE-221 00 Lund  
Sweden

brand@brand.lth.se  
<http://www.brand.lth.se/english>

Telephone: +46 46 222 73 60  
Fax: +46 46 222 46 12

---

## TABLE OF CONTENTS

TABLE OF CONTENTS.....	1
SAMMANFATTNING.....	3
SUMMARY .....	5
LIST OF SYMBOLS.....	7
1. INTRODUCTION.....	9
2. MAXIMUM EXTERNAL HEAT FLUX .....	11
3. FLAME-SPREAD OVER SOLIDS.....	17
4. THE WPI FIRE/CODE.....	23
5. SENSITIVITY ANALYSIS ON INPUT PARAMETERS .....	29
6. TRANSLATION FROM BENCH SCALE TO FULL SCALE DATA.....	33
7. COMPARISON WITH EXPERIMENTAL DATA.....	37
8. CONCLUSION AND RECOMMENDATIONS ON FURTHER WORK.....	41
REFERENCES.....	43
APPENDIX A. TIME TO IGNITION AND EXTERNAL HEAT FLUX.....	45
APPENDIX B. INFLUENCE OF EXTERNAL HEAT FLUX.....	49
APPENDIX C. INPUT DATA FILE TO <i>THIMES</i> .....	53
APPENDIX D. COMPARISON OF RESULTS .....	55
APPENDIX E. NOMENCLATURE IN THE WPI/FIRE CODE.....	57
APPENDIX F. THE SOURCE CODE TO THE SUBROUTINE <i>WPLUM</i> .....	59
APPENDIX G. MODEL A.....	63
APPENDIX H. MODEL B .....	65
APPENDIX I. THE SOURCE CODE TO <i>THIMES</i> .....	77



## SAMMANFATTNING

Effekten som utvecklas vid en rumsbrand är en av de mest grundläggande indata parametrarna till en zonmodell. Kan effektutvecklingen beräknas är det vidare möjligt att även beräkna t.ex. temperaturer, brandgaslagrets höjd och strålningen från det övre brandgaslagret. Då det brinner i ett rum är det möjligt att den initiella branden sprider sig till brännbara ytmaterial på väggarna. Då dessa också börjar brinna kommer det att ge ett tillskott till den totala effekten som utvecklas i rummet. Detta tillägg är svårt att beräkna.

Målet med detta projekt är att integrera Baroudi/Kokkalas flamspridnings modell in i WPI/Fire Code, som är en zonmodell. Detta skulle ge användaren av zonmodellen en möjlighet att endast behöva ange effektutvecklingen för den initiella branden, WPI/Fire Code tar sedan själv hänsyn till tillägget från flamspridningen.

För att kunna integrera flamspridningsmodellen in i zonmodellen måste man bortse från det faktum att den externa strålningen kommer att påverka faktorer som väggmaterialets effektutveckling per ytenhet och dess tid till antändning. Med andra ord måste ett maximalt tillåtet värde på den externa strålningen bestämmas. I denna rapport har ett värde på 10 % använts som tillåten osäkerhet. Detta är samma osäkerhet som vid experimentella mätningar. Vidare presenteras en metod som visar hur ett värde på den maximalt tillåtna strålningen utifrån en bestämd osäkerhet kan härledas. Beräkningar ger att den maximalt tillåtna externa strålningen sätts till  $5 \text{ kW/m}^2$ . Vid denna strålningsnivå kommer brandgastemperaturen i det övre lagret att ligga runt  $300 \text{ }^\circ\text{C}$ . Resultaten från zonmodellen då strålningsnivån eller brandgastemperaturen når dessa nivåer bör granskas kritiskt.

Eftersom flamspridningsmodellen bland annat ger effektutvecklingen som utdata måste ett par justeringar göras i denna innan den integreras i WPI/Fire Code. WPI/Fire Code använder massavbrinning som indata i stället för effektutveckling. Som följd av detta så beräknades massavbrinningen via effektutvecklingen i flamspridningsmodellen. Massavbrinningen sattes sedan i en tabell tillsammans med simuleringstiden. Denna tabell gavs som enda utdata från flamspridningsmodellen till WPI/Fire Code. Vidare ändrades Baroudi/Kokkala modellen om från att vara ett exekverbart program till en subrutin som kallas av WPI/Fire Code.

Ett försök att förbättra plymmodellen i WPI/Fire Code gjordes eftersom flamspridningsmodellen förutsätter att den initiella branden sker intill en vägg. En ny subrutin som räknar på plymen skrevs. Tester visade att sub-modellen fungerade fint så länge den inte kopplades samman med zonmodellen, men när den integrerades i zonmodellen fungerade den inte som förväntat. Inga ytterligare försök gjordes för att korrigera detta fel, på grund av att det är tidskrävande och programmeringsmässigt svårt.

Den mest omfattande förändringen av zonmodellen är en sub-rutin som kallas WFIRE. WFIRE interpolerar fram rätt värde på massavbrinningen ur den tabell som flamspridningsmodellen producerar.

När beräknade resultat jämförs med experimentella data måste ett par justeringar göras i flamspridningsmodellen för att den ska passa scenariot som den jämförs med. För att ta reda på

vilka parametrar som har störst betydelse utsattes de för en känslighetsanalys. Parametrarna som analyserades är:

- Den initiella flamhöjden
- Tid till antändning
- Flamhöjdskonstanten

Vidare analyserades data från olika strålningsnivåer i konkalorimetern. Detta innebar:

- Olika kombinationer av kondata, dvs tid till antändning och effektutveckling per areaenhet vid 25 och 50 kW/m<sup>2</sup>

Resultaten från känslighetsanalysen visar att fokuseringen bör ligga på följande parametrar då beräknade resultat jämförs med experimentella data:

- Flamhöjdskonstanten
- Data från konkalorimetern, dvs tid till antändning och effektutveckling per ytenhet

Två olika modeller användes för att jämföra programmet med experiment. Modell A jämför beräknade resultat med experimentella data från en fritt brinnande vägg. Modell B jämför data från ISO 9705 Room Corner Test med beräknade resultat. Modell A använder kondata från en strålningsnivå på 50 kW/m<sup>2</sup> som indata. Resultaten visar att om denna typen av kondata ska användas som indata måste värdet på flamhöjdskonstanten sänkas till en orimligt låg nivå. Modell B visar däremot väldigt bra överrenstämmelse med experimentell data från ISO 9705 Room Corner Test, speciellt för trä-baserade material.

Ett syfte med en zonmodell är att temperaturen i övre brandgaslagret ska kunna beräknas. Då modell B utvärderades jämfördes inte bara effektutvecklingen utan även temperaturen i övre brandgaslagret. Resultaten visar att WPI/Fire Code generellt underskattade temperaturen. Detta fenomen kan förklaras med plymmodellen. Om plymmodellen överskattar massavbrinningen kommer temperaturen i övre brandgaslagret att bli lägre. Detta problem kan lösas genom att en ny plymmodell integreras i zonmodellen.

Utvärderingen av modell B visar också att en temperatur på 300 °C, temperatur begränsningen på flamspridningsmodellen, uppnås samtidigt som övertändning sker i ISO 9705 rummet. Detta betyder att WPI/Fire Code kan användas till att utvärdera hur nya material kommer att uppföra sig i Room Corner Test, dvs om de går till övertändning eller inte.

Även om WPI/Fire Code kan beräkna effektutvecklingen pga flamspridning korrekt är det inte rätt att påstå att flamspridningsmodellen är integrerad i zonmodellen. En fullständig integration skulle betyda att massavbrinningen beräknas vid varje tidssteg och inte interpoleras fram i en massavbrinningstabell som sträcker sig över hela simuleringstiden som resultatet av detta projekt är. Resultaten kommer dock bli identiska i de båda fallen.

## SUMMARY

The heat release rate developed in an enclosure is one of the basic input data to a computational fire model. If the HRR is known, it is further possible to calculate e.g. gastemperatures, layer heights and radiation from the hot layer. When the burning occurs in an enclosure, the fire might spread across any combustible lining materials present and give an addition to the HRR developed in the room. This addition is hard to calculate.

The goal of this project is to incorporate a flame-spread model, the so-called Baroudi/Kokkala algorithm, into the WPI/Fire Code. This would allow the user to only specify the initial burning object and then would the WPI/Fire Code calculate the addition given by the flame-spread.

To be able to make an easy integration of the Baroudi/Kokkala flame-spread algorithm into the WPI/fire code and to neglect the fact that the time to ignition and the HRR varies with different external radiation, i.e. allowing a variance from a more exact result, a maximum external radiation allowed must be determined. A maximum allowed percentage value of uncertainty is set to 10%, which is the same uncertainty as in measurements. A method that calculates an external heat flux allowed from this percentage value is presented. The calculations gives the mean value of the maximum external heat flux allowed as  $4.75 \text{ kW/m}^2$ , the final value is set to be  $5 \text{ kW/m}^2$ . With a  $\dot{q}_{ext}''$  of  $5 \text{ kW/m}^2$  the maximum temperature will be around 550 K, i.e. roughly  $300 \text{ }^\circ\text{C}$ . The results from the zone model should be critically looked upon when the upper layer temperature reaches  $300 \text{ }^\circ\text{C}$  or the external heat flux reaches  $5 \text{ kW/m}^2$ .

Since the output from Baroudi/Kokkala algorithm is the HRR (among other things) some changes had to be made to the Baroudi/Kokkala algorithm before integrating it into the WPI/Fire Code. First of all, the WPI/Fire Code uses mass-loss rate as input instead of HRR. As a result of this the mass-loss rate from the burning wall was calculated via the HRR in the Baroudi/Kokkala algorithm and then put in a table, together with the simulation time, serving as the only output from the flame-spread model. Further the Baroudi/Kokkala algorithm, which is a executable program, was turned into a subroutine called by the main program in the WPI/Fire Code

An attempt was made to improve the plume model in the WPI/Fire Code since the flame-spread algorithm assumes that the burning occur against a wall. A new plume sub-model was written. Tests showed that the plume sub-model worked properly when used outside the WPI/Fire Code. However, when integrated, the plume sub-model did not work as it should. No further attempt was made to correct this problem due to the need of programming skills and the size and complexity of the WPI/Fire source code.

The most extensive addition to the WPI/Fire Code was a subroutine called WFIRE. WFIRE interpolates the correct mass-loss rate from the table (called ZASSA in the WPI/Fire Code) derived from the flame-spread subroutine.

When comparing calculated results with experimental data some corrections to the flame-spread model had to be made so that the model fits the scenario that it is tested against. To be able to know which parameters to focus on the input parameters to the flame-spread model were exposed to a sensitivity analysis. The parameters analyzed are:

- Initial flame height
- Time to ignition
- Flame height correlation factor

Further, an analysis of the influence from cone calorimeter data at different irradiance levels was carried out. This analysis includes:

- Combinations of cone calorimeter data, i.e. time to ignition and HRR per unit area, at 25 kW/m<sup>2</sup> and 50 kW/m<sup>2</sup>

The sensitivity analysis shows that the parameters to focus on when comparing simulated results and experimental results are:

- flame height correlation factor and
- cone calorimeter data i.e. time to ignition and HRR

Two different models are used when evaluating the code against experiments. Model A compares data from a free burning wall with data calculated by the WPI/Fire Code and Model B compares data from the ISO 9705 Room Corner Test with data calculated by the WPI/Fire Code. Model A uses cone data from an irradiance level of 50 kW/m<sup>2</sup>. The results show that if this type of cone data is going to be used, the flame height correlation factor has to be lowered to an unrealistically low value. Model B, on the other hand, show very good agreement with the experimental data from the Room Corner Test, especially when evaluating wood based materials.

One purpose of a zone model is that you are able to calculate the upper layer temperature in a compartment. So when comparing the calculated results with the Room/Corner Test, Model B, the upper layer temperature was also calculated and compared. The WPI/Fire Code generally underestimates the upper layer temperature. This phenomenon can be explained by the plume-model. If the plume-model overestimates the mass-loss rate, the upper layer temperature will be lower. This problem might be solved if a wall-plume subroutine is successfully integrated.

The evaluation of Model B also shows that the upper layer temperature of 300 °C, the temperature limitation of the flame-spread model, is reached at roughly the same time as the theoretical maximum HRR for flashover in the ISO 9705 room is reached. This states that the WPI/Fire model can be used to analyze a new materials behavior in the ISO 9705 test, does the material reach flashover or not?

Even though the WPI/Fire Code is able to calculate HRR from flame-spread correctly it is not correct to say that the flame-spread model is fully integrated into the WPI/Fire Code. A complete integration would be that the mass-loss rate from flame-spread is calculated at each time step and not for the whole simulation period and then interpolated for the correct time step, as the result of this project is. However, the results would be the same in both cases.

## LIST OF SYMBOLS

$\Delta H_C$	Heat of Combustion (KJ/Kg)
$k$	Thermal conductivity of the fuel (KW/mK)
$K$	Constant in flame height correlations ( $m^2/kW$ )
$k\rho c$	Apparent thermal inertia ( $kW^2s/m^4K^2$ )
$\dot{m}$	Mass loss rate of the fuel (Kg/s)
$n$	Exponential constant in flame height correlations (-)
$\dot{Q}$	Energy release rate (kW)
$\dot{Q}_b$	Energy release rate of the burner (kW)
$\dot{Q}''_{cone}$	Energy release rate per unit area of the fuel in the cone ( $kW/m^2$ )
$\dot{Q}_{tot}$	Total energy release rate (kW)
$\dot{q}''_{ext}$	External heat flux per unit area ( $kW/m^2$ )
$\dot{q}''$	Heat flux per unit area ( $kW/m^2$ )
$t_{ig}$	Time to ignition (s)
$t_p$	Time (s)
$T_0$	Initial temperature (K)
$T_{ig}$	Ignition temperature of the fuel (K)
$T_{max}$	Maximum temperature (K)
$T_s$	Surface temperature (K)
$V$	Velocity (m/s)
$W$	Width (m)
$x_f$	Flame height (m)
$x_{fb}$	Flame height from the burner (m)
$x_p$	Height of the pyrolysis front (m)
$x_{p0}$	Initial height of the pyrolysis front (m)
$Y_{max}$	Height of the wall (m)
$\chi$	Combustion efficiency (-)
$\sigma$	Stefan Boltzmann constant ( $W/m^2K^4$ )



## 1. INTRODUCTION

This document reports the results from a final year project at the Bachelor of Science degree program in Fire Protection Engineering at Lund University, Sweden. The project was carried out in close cooperation with the Worcester Polytechnic Institute, Worcester, Massachusetts USA. Supervisors for the project have been Tekn. Dr Björn Karlsson at Lund University and Professor Jonathan Barnett at Worcester Polytechnic Institute.

### 1.1 BACKGROUND

Computational fire modeling is a valuable tool for the Fire Safety Engineer. However, it is sometimes very hard to give the correct input data to the computer program. The heat release rate (HRR) developed in the enclosure is one of the basic input data to a computational fire model. If the HRR is known, it is further possible to calculate e.g. gastemperatures, layer heights and radiation from the hot layer. These data can be used to analyze the human and structural safety in a building. When a Fire Safety Engineer analyses a fire in a building, he/she characterizes the fire by its HRR curve. These curves are often the product of a free burning test. It becomes more difficult to calculate the HRR curve when the burning occurs in an enclosure. The fire might spread across any combustible lining materials present and it will give an addition to the HRR developed in the room. This addition is hard to calculate and the fire will be underestimated if only the HRR curve for the initial burning object is used.

The WPI/Fire Code is a computational zone-type fire model developed at Worcester Polytechnic Institute, Massachusetts. The user of the WPI/Fire Code had 3 different ways to describe the fire, none of them taking flame spread on surfaces and fire growth into account. The goal for this project is to incorporate a flame-spread model into the WPI/Fire Code so that the user has an option to simulate wall fires.

This project has been carried out in two phases:

*Phase 1.* At the Worcester Polytechnic Institute the Baroudi/Kokkala flame-spread algorithm was incorporated into the WPI/Fire Code. The extent of this work in terms of time and effort is very hard to show in this report, due to the very large size of the source code and also due to consideration for the reader of this report. The changes and additions made will however be notified in plain language.

*Phase 2.* At Lund University the code was validated against experiments. This work is documented in this report.

### 1.2 Limitations

The result of this work will be an enhanced zone type fire model, which is of particular value in evaluating life safety. The project focuses on the early stage of a fire. This is because the flame-spread model does not take into account the incident flux from other burning objects or the hot layer. This leads to the following limitations:

- The flame-spread model will only be valid until the temperature of the hot layer reaches a maximum value. At higher temperatures the radiation from the hot layer to the walls will affect the time to ignition and the HRR. This maximum temperature will be determined in Chapter 2.
- The model will only be valid for external heat flux levels below a critical value. Heat fluxes above the critical value will have the same effects as explained above. An appropriate value for this critical heat flux will be determined in Chapter 2.
- Only scenarios similar to one involving a burner located against a wall or in a corner will be taken into account.

### **1.3 Overview of this thesis**

Chapter 2 discusses the influence that the external heat flux has on the results and how much external heat flux is tolerable until it has an effect on the flame-spread. A value on the maximum tolerable level will be determined.

The thermal theories for upward flame-spread will be discussed in Chapter 3. This chapter also includes a discussion on the Baroudi/Kokkala algorithm and the changes to the algorithm that were necessary in order to incorporate it into the zone model.

The zone model used for the integration process was the WPI/Fire Code. A general discussion on zone models, and a more specific explanation of the WPI/Fire Code is given in Chapter 4. This chapter also discusses the adjustments that were made to the source code during the integration process.

Chapter 5 contains a simple sensitivity analysis that was carried out on the input parameters to the flame-spread model.

Chapter 6 discusses the issue of translating bench scale data to full-scale data. This chapter also contains a description of the models that were used when evaluating the code.

The results from comparisons between experiments and computer-calculated data are shown and discussed in Chapter 7.

The final chapter, Chapter 8, includes a conclusion and some recommendations for further work.

## 2. MAXIMUM EXTERNAL HEAT FLUX

This chapter discusses the influence the external heat flux has on flame-spread. A method that calculates the maximum tolerable value on the external heat flux is introduced. Finally the results from the calculations are presented and a maximum tolerable upper layer temperature is derived.

### 2.1 General

When a material is exposed to an external radiation, the surface temperature will rise and cause the material to pyrolyse. After some time the fuel/air mixture above the material reaches the lower flammability limit and the material ignites, producing heat. Depending on the amount of external radiation the material will experience different times to ignition and heat release rates. A higher radiation will result in a shorter time to ignition and a higher HRR. One way to measure this is by using the Cone Calorimeter /Babrauskas et al. 1988/, Figure 2.1 below.

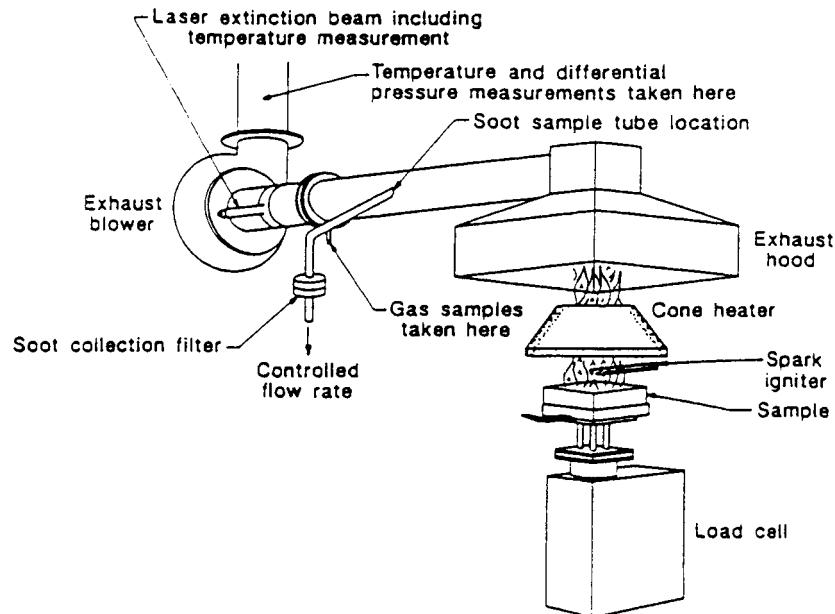


Figure 2.1. Schematic view of the Cone Calorimeter /Karlsson 1992/

In the Cone Calorimeter a square sample of the material is exposed to a radiant flux, typically within a range of  $25 - 75 \text{ kW/m}^2$ . A spark igniter is used as pilot ignition. The HRR per unit area is measured by using the oxygen consumption method /Janssens 1991/ and the time to ignition is achieved from plotting the HRR vs. time and defining the time to ignition as e.g. the time when the HRR reaches  $50 \text{ kW/m}^2$ . In Figure 2.2 below, two plots at different irradiance levels are shown to illustrate the fact that the HRR per unit area and the time to ignition varies with different irradiance levels.

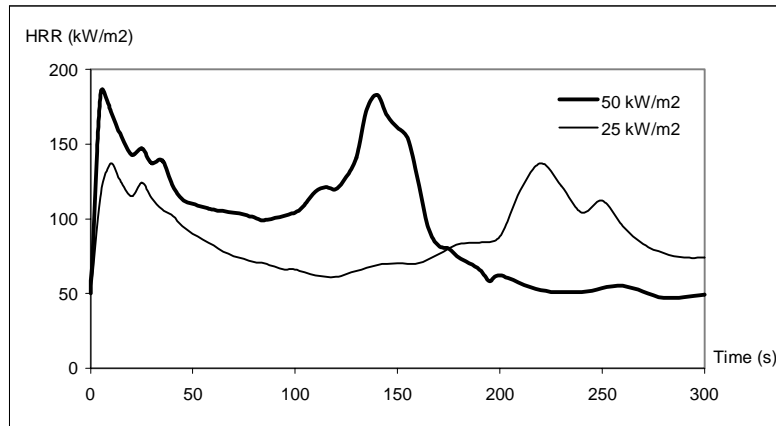


Figure 2.2. Cone Calorimeter plots at two different irradiance levels for a specific material.

The Baroudi/Kokkala flame-spread algorithm /Baroudi et al. 1997/ is developed on the basis of a wall fire in the open, i.e. it does not take external radiation, other than from the flame, into account. However this is not the case when the burning occurs in an enclosure. The hot layer emits radiation and causes the material in the walls to warm up. This will result in a shorter time to ignition and a higher HRR per unit area; i.e. the flame-spread velocity will increase.

When calculating the HRR from a burning wall you need the time to ignition and the HRR per unit area from the Cone Calorimeter as input. If you compare these two inputs you find that it is the time to ignition that has the most decisive effect on the result. Therefore it is most common that the emphasis is put on calculating the correct time to ignition connected with the external radiation. Karlsson /Karlsson 1992/ approached this by using the heat transfer theory with constant external radiation /Carlslaw et. al 1959/ and calculating a surface temperature. Then the time to ignition is calculated using Equation 2.1 /Carlslaw et. al 1959/ below for each time step. Equation 2.1 is arrived by solving the general heat conduction equation with very simple boundary conditions.

$$t_{ig} = \frac{k\rho c * \pi * (T_{ig} - T_s)}{4 * (\dot{q}_{ext}'' )^2} \quad [2.1]$$

Here  $T_{ig}$  is the ignition temperature,  $T_s$  is the surface temperature,  $\dot{q}_{ext}''$  is the external radiation and  $k\rho c$  is the thermal inertia of the material.

To be able to make an easy integration of the Baroudi/Kokkala algorithm into the WPI/fire code and to neglect the fact that the time to ignition and the HRR varies with different external radiation, i.e. allowing a variance from the more exact result, a maximum external radiation allowed must be determined. The method which is used and the achieved results are presented in the two following sections.

## 2.2 Method

Baroudi et al. /Baroudi et al./ developed a flame-spread computer algorithm, *Thimes*, based on the theories developed by Karlsson /Karlsson 1992/. The *Thimes* algorithm uses, among other things, Cone Calorimeter data at an irradiance of  $25 \text{ kW/m}^2$  as input.

To determine the maximum external radiation allowed one must first set a limit on how much the result may vary (percentage difference) from the original values (with the HRR and the time to ignition at  $25 \text{ kW/m}^2$ ). As mentioned above the emphasis is put on the time to ignition. The HRR per unit area is fixed and then by varying the time to ignition one gets different plots (HRR vs. time) as shown in Figure 2.3 below. If the percentage difference, between the plot with the original values and the plot with the new time to ignition, is under the set limit an external radiance connected with this new time to ignition can be calculated. This is done by using Cone Calorimeter data at different irradiance levels e.g.  $25 \text{ kW/m}^2$  and  $50 \text{ kW/m}^2$ . The following example will illustrate the method.

Example:

The material used in this example, see Table 2.1 below, is particle board on mineral wool, one of the materials that was used for developing the Baroudi/Kokkala algorithm.

Material:	Time to ignition (s)	
	$25 \text{ kW/m}^2$ irradiance	$50 \text{ kW/m}^2$ irradiance
11 mm particle board on 50 mm mineral wool	106	34

Table 2.1. Material used in example

In this example the percentage difference limit in HRR is set to 5 %. The different plots received from *Thimes* are shown in Figure 2.3 below.

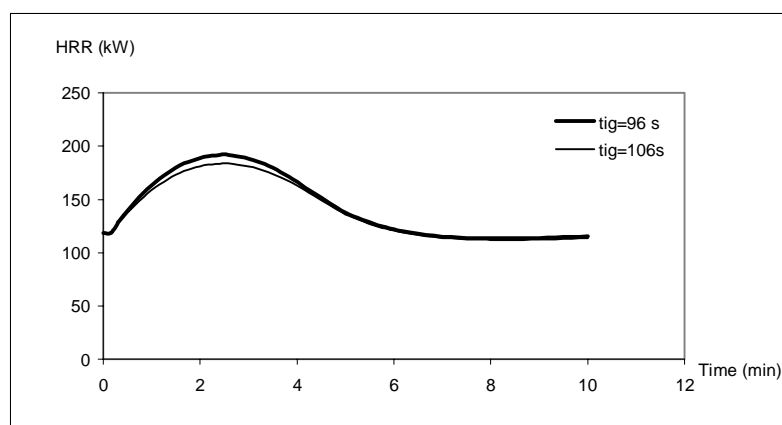


Figure 2.3. Plots from *Thimes* at different time to ignition for a particle board

The calculated difference between the two plots is shown in Figure 2.4 below. The limit of 5 % is never exceeded and the time to ignition **96** seconds can therefore be used to calculate the external radiation.

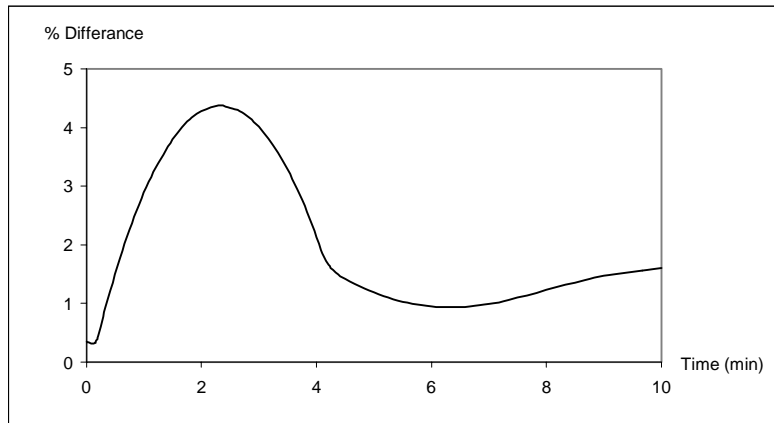


Figure 2.4. Calculated difference between plots

Assuming linear relation between the to time to ignition in Table 2.1, the external radiation matching the time to ignition 96 seconds will be as follows:

$$\dot{q}_{ext}'' = 25 + (25 - 50)/(106 - 34) * (96 - 106) = \mathbf{28.5 \text{ kW/m}^2}$$

Thus the maximum external radiation allowed will be  $28.5 - 25 = \mathbf{3.5 \text{ kW/m}^2}$ , with the chosen percentage limit of 5 %. The matching  $\dot{q}_{ext}''$  can also be derived from a  $t_{ig}$  vs.  $\dot{q}_{ext}''$  plot as shown in Appendix A. However, this method might not give the same result since the actual relationship between  $t_{ig}$  and  $\dot{q}_{ext}''$  is not linear. The later method is preferred, since it is more correct.

This procedure is then repeated for available Cone Calorimeter data and a mean value is calculated, giving an indication of the magnitude of the percentage limit representing all materials.

### 2.3 Percentage difference limit

The HRR measured in a calorimeter is connected with an uncertainty. Björn Sundström /Sundström 1990/ and Martin Dahlberg /Dahlberg 1992/ gives this uncertainty as 10 % (furniture calorimeter) and 8 – 16 % (industry calorimeter) respectively. Since the calorimeter which is used in the tests, that are of interest in this work (Room/Corner Test), is a furniture calorimeter, we choose to use the uncertainty level of 10 % (this value is also within the range for the industry calorimeter given in /Dahlberg 1992/)

The percentage limit mentioned in the sections above is set depending on how accurate the user wants the calculated results to be. A reasonable value for the percentage limit is the same as the uncertainty of the measured HRR. Thus the percentage limit is set equal to the value of the uncertainty in the measurements, i.e. the percentage limit used is **10 %**.

## 2.4 Results

The materials that are tested to come up with the maximum external radiation allowed are part of the Eurefic program /Wickström 1993/ and were used in the development of *Thimes*. These materials are presented in Table 2.2 below. A  $t_{ig}$  vs.  $\dot{q}_{ext}''$  plot of these materials is shown in Appendix A.

Material (Eurefic nr.)	Time to ignition at 25 kW/m <sup>2</sup> (s)	Time to ignition at 35 kW/m <sup>2</sup> (s)	Time to ignition at 50 kW/m <sup>2</sup> (s)
Ordinary plywood (E2)	143	46	26
Textile wall covering (E3)	132	57	20
Plastic faced steel sheet (E5)	85	80	34
Faced rockwool (E7)	5	7	10
PUR foam (E9)	17	25	33
PVC wall carpet (E10)	39	22	14

Table 2.2. Materials tested and their time to ignition at different heat fluxes

From the percentage difference plots in Appendix B and the  $t_{ig}$  vs.  $\dot{q}_{ext}''$  plots in Appendix A we get the results listed in Table 2.3 below:

Material (Eurefic nr.)	Time to ignition giving a percentage difference < 10 % (s)	Maximum additional heat flux allowed (kW/m <sup>2</sup> )
Ordinary plywood (E2)	135	2.5
Textile wall covering (E3)	124	2.5
Plastic faced steel sheet (E5)	80	6.8
Faced rock wool (E7)	9	5
PUR foam (E9)	27	7.2
PVC wall carpet (E10)	37	4.5

Table 2.3. Results for all the tested materials

The mean value of the maximum external heat flux allowed is 4.75 kW/m<sup>2</sup>, the final value is set to be 5 kW/m<sup>2</sup>.

## 2.5 Upper layer temperature

Since there are no other burning objects in the simulations, the additional heat flux will mainly come from the hot layer. Thus the maximum external heat flux will result in a maximum upper layer temperature. When the temperature in the simulation of the fire reaches this maximum temperature the simulation results should be critically analyzed.

Assuming a uniform temperature in the upper layer, an emission factor of 1, a view factor of 1 and neglecting the re-radiation from the upper walls and ceiling, we get the following expression

for the maximum temperature (the assumptions made will result in a underestimate of the temperature):

$$T_{\max} = \left( \frac{\dot{q}_{ext}''}{\sigma} \right)^{1/4} \quad [2.2]$$

where  $\sigma$  is the Stefan-Boltzmann constant =  $5.67 \cdot 10^{-8}$  [W/m<sup>2</sup>K<sup>4</sup>].

With a  $\dot{q}_{ext}''$  of 5 kW/m<sup>2</sup> the maximum temperature will be around 550 K, i.e. roughly 300 °C. The temperature limit mentioned in Chapter 1 would therefore be 300 °C.

## 2.6 Conclusion

The flame-spread velocity will increase with increasing external heat flux and finally reach a level where the results become unrealistic. When the external heat flux reaches 5 kW/m<sup>2</sup> or the upper layer temperature reaches approximately 300 °C the flame-spread model overestimates the HRR by approximately 10 %. This is a tolerable level since the accuracy of experimental measurements is not any better. The results given by the flame-spread algorithm should be looked upon as reasonable as long as the upper layer temperature is below 300 °C.

These results indicate that the model can be used to simulate the early stage of the fire and it might be a valuable tool when evaluating life safety.

### **3. FLAME-SPREAD OVER SOLIDS**

In the beginning of this chapter flame-spread will be discussed generally. Further is the Baroudi/Kokkala flame-spread algorithm, derived from the Karlsson model, explained. Finally are all the adjustments made to this model presented.

#### **3.1 General on flame-spread**

The many theories on flame-spread that have been presented in the past can be divided into two different groups: theories that consider chemical kinetics and regard flame temperature and radiation as variables, and secondly those who consider radiation and flame temperature as constants, i.e. only considering energy conservation (so called thermal theories). /Karlsson 1992/

The flame-spread is highly dependent on the orientation of the burning solid and the present wind conditions. If the material is vertically orientated and the ignition occurs at the bottom, the flame-spread will progress in the same direction as the rising air (wind aided flame-spread). On the other hand, if the ignition occurs at the top the flame will spread in the opposite direction to the wind (opposed flame-spread). The latter flame-spread is approximately 10 – 100 times slower than the wind aided flame-spread.

The type of flame-spread that is used in the Karlsson model /Karlsson 1992/ is the wind aided thermal theory. Since wind aided flame-spread is much faster than opposed flame-spread the assumption that the propagating pyrolysis front is of constant width is made, i.e. neglecting opposed flame-spread.

The following sections will give a quick review of the thermal wind aided model as presented by Karlsson /Karlsson 1992/ and further developed by Baroudi/Kokkala /Baroudi et al./; using the model and changes made to the model.

#### **3.2 General on thermal wind aided flame-spread**

To be able to come up with a mathematical expression for the HRR from a burning wall, initially ignited by a burner, some approximations have to be made. The main approximations are /Karlsson 1992/:

- 1) The material is considered thermally thick, homogenous and its thermal properties are constant with temperature
- 2) The material is sufficiently thick so that no burn out occurs
- 3) The flame length (see Figure 3.1) depends on the power of the HRR
- 4) The radiation from the flame is constant over the heating region (see Figure 3.1) and zero above it
- 5) Steady-state initial conditions, i.e. constant burner output

A schematic view of the wall configuration is shown in Figure 3.1. If convective and radiative cooling is ignored the following expression for ignition temperature is used /Carlslaw et. al 1959/

$$T_{ig} - T_0 = \frac{2\dot{q}_{ext}''}{\sqrt{\pi}} \sqrt{t_{ig}} \sqrt{k\rho c} \quad [3.1]$$

where  $t_{ig}$  denotes the time to ignition. This equation is based on the general heat conduction equation, the initial condition  $T(t,0) = T_0$  and the boundary condition at  $y=0$  as follows:

$$\dot{q}''(0,t) = \dot{q}_{ext}'' = -k \frac{dT}{dy} \quad [3.2]$$

If we rewrite Equation [3.1] and replace the time to ignition with the velocity of the pyrolysis front divided by the heating distance  $x_f - x_p$  (see Figure 3.1 below) we arrive at an expression for the velocity of the pyrolysis front.

$$V = \frac{4(\dot{q}_{ext}'')^2 (x_f - x_p)}{\pi k \rho c (T_{ig} - T_0)^2} \quad [3.3]$$

This equation can also be expressed as

$$V(t) = \frac{x_f - x_p}{t_{ig}} = \frac{dx_p}{dt} \quad [3.4]$$

where  $t_{ig}$  is derived from Equation [3.1].

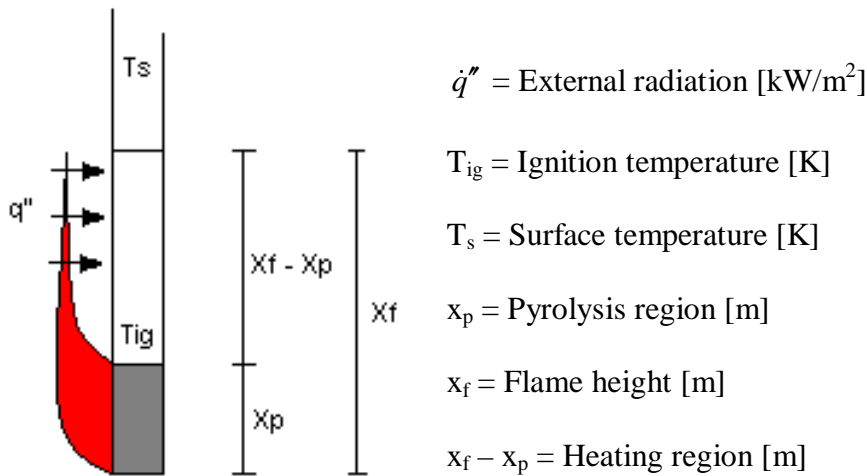


Figure 3.1. Wall section, radiation from flame assumed to be constants over  $(x_f - x_p)$

The variables  $x_f$  and  $x_p$  have to be further expressed in order to get a complete expression for the velocity of the pyrolysis front,  $V(t)$ . The height of the pyrolysis front as a function of time is given as:

$$x_p(t) = x_{p0} + \int_0^t V(t_p) dt_p \quad [3.5]$$

where  $t_p$  is the dummy variable of integration and  $x_{p0}$  is the pyrolysis front at the initial timestep  $t = t(0) = 0$ .

As mentioned earlier the flame height  $x_f$  depends on the power of the HRR and is on the form

$$x_f = K(\dot{Q}_{tot}(t))^n \quad [3.6]$$

where  $\dot{Q}_{tot}(t)$  is the total HRR at time  $t$  and  $K$  (flame height correlation factor) and  $n$  are constants derived from experiments. These constants are dependent on the choice of scenario, i.e. if the fire occurs on a wall or in a corner. /Karlsson 1992/

The initial pyrolysis height is calculated as the flame height from the burner. This flame height is thus given as:

$$x_{p0} = x_{fb} = K(\dot{Q}_b)^n \quad [3.7]$$

When the material behind the burner is ignited the time is taken to be  $t=0$ . The flame height at  $t=0$ , termed  $x_{f0}$ , is given by Equation [3.6] with the total HRR as the HRR from the burner and the initially burning material. Thus the flame height at  $t=0$  is

$$x_{f0} = K(\dot{Q}_b + x_{p0}W\dot{q}_{cone}''(0))^n \quad [3.8]$$

where  $W$  is the width of the pyrolysis front, as mentioned earlier assumed to be the same as the burner width, and  $\dot{q}_{cone}''(0)$  is the HRR per unit area from the material at ignition.

The total HRR at any time  $t>0$  can now be expressed as

$$\dot{Q}_{tot}(t) = \dot{Q}_b + x_{p0}W\dot{q}''(t) + W\int_0^t \dot{q}''(t-t_p)V(t_p)dt_p \quad [3.9]$$

where  $t_p$  is a dummy variable of integration. The three terms on the right hand side are the burner output, the HRR from the initial ignited wall area and the HRR from the flame-spread respectively.

Going back to the main equation for the flame-spread velocity, Equation [3.4], we can now express the flame-spread velocity by substituting the flame height,  $x_f$ , with Equation [3.6] and using Equation [3.9] as the expression for the total HRR. And further expressing the pyrolysis height using Equation [3.5] we arrive at the following equation, which is a Volterra integral equation of the second kind /Karlsson 1992/.

$$V(t) = \frac{1}{t_{ig}} \left[ K \left( \dot{Q}_b + x_{p0} W \dot{q}''(t) + W \int_0^t \dot{q}''(t-t_p) V(t_p) dt_p \right)^n - \left( x_{p0} + \int_0^t V(t_p) dt_p \right) \right] \quad [3.10]$$

where the two terms in the larger bracket are  $x_f$  and  $x_p$  respectively.

Karlsson and Thomas /Karlsson et al 1990/ solved this analytically with Laplace transformations, arriving at an expression for the flame-spread velocity which then can be used in Equation [3.9] to calculate the HRR. Karlsson /Karlsson 1992/ developed this further and tested the model against experiments. The flame-spread algorithm used in this project, the Baroudi/Kokkala, solves this in a different way. The model will be further described in the following section.

### 3.3 The Baroudi/Kokkala Flame-spread Algorithm

Instead of solving Equation [3.4] using the Volterra type integral in Equation [3.10], Baroudi et al integrates Equation [3.4] directly using the first order forward Euler method /Edward et al 1956/. Thus Equation [3.4] becomes:

$$x_p(t_{i+1}) = \left( 1 - \frac{\Delta t_{i+1}}{t_{ig}} \right) x_p(t_i) + \left( \frac{\Delta t_{i+1}}{t_{ig}} \right) x_f(t_i) \quad [3.11]$$

where  $\Delta t_{i+1} = t_{i+1} - t_i$ .

The velocity of the pyrolysis front at  $t = t_{i+1}$  can be expressed as the mean velocity between  $x_p(t_{i+1})$  and  $x_p(t_i)$ , shown in Equation [3.12].

$$\frac{dx_p(t_{i+1})}{dt} \approx \frac{x_p(t_{i+1}) - x_p(t_i)}{\Delta t_{i+1}} \quad [3.12]$$

The integral in Equation [3.9] is approximated using the trapezoidal integration rule /Edward et al 1956/ and thus the total HRR can be written as:

$$\dot{Q}_{tot}(t) = \dot{Q}_b + x_{p0} W \dot{q}''(t) + W \sum_{p=1}^{p=i} \dot{q}''(t-t_p) \frac{x_f(t_p) - x_p(t_p)}{t_{ig}} \omega_p \quad [3.13]$$

where  $t_{p=1} = t(0)$  and  $t_{p=i} = t$ . The weight  $\omega_p$ , which comes from the trapezoidal integration, equals  $\Delta t_{i+1}/2$  except when  $p=1$  and  $p=i$  where  $\omega_p$  equals  $\Delta t_{i+1}$ . This is the equation used in the numerical model *Thimes* along with the equations for the flame height and the pyrolysis front addressed in the section above. There is also the addition that when the flame height is shorter than the pyrolysis height the flame height is set equal to the height of the pyrolysis front, i.e.

$$\text{when } x_f(t_{i+1}) < x_p(t_{i+1}) \text{ then set } x_f(t_{i+1}) = x_p(t_{i+1})$$

This accounts for the coincidence of the flame and pyrolysis heights during the periods when the flame is receding /Baroudi et al 1997/.

### 3.4 Using the Baroudi/Kokkala Algorithm

This model is developed and “fine tuned” under certain conditions e.g. the Cone Calorimeter data is taken from both 25 kW/m<sup>2</sup> and 50 kW/m<sup>2</sup>. The following list contains the conditions under which the model has been developed:

- Cone Calorimeter data used in the flame-spread algorithm, time to ignition and HRR per unit area, is taken from an irradiance level of 25 kW/m<sup>2</sup>.
- The parameters K (flame height correlation factor) and n are set to  $0.65 \cdot 10^{-5} \text{ m}^2/\text{W}$  and 1 respectively.
- The initial pyrolysis height is set to 0.2 m when using a 100 kW burner.
- When the calculation of the HRR is finished and the results are compared to experiments, a shift in the time scale has to be made to illustrate the initial ignition time. This time is taken as the time to ignition in the Cone Calorimeter at 50 kW/m<sup>2</sup>.

The input data file to *Thimes* is shown in Appendix C.

### 3.5 Adjustments to the Baroudi/Kokkala Algorithm

The HRR is calculated in the WPI/Fire Code via the mass loss rate from the burning object. The mass loss rate is handled in the two subroutines TMGAS and PYRO depending on what kind of fire the user has chosen, i.e. TMGAS for gas burner and PYRO for pool fire or growing fire. Since the output from *Thimes* is the HRR (among other things) some changes had to be made to the Baroudi/Kokkala algorithm before integrating it into the WPI/Fire Code. The mass loss rate from the wall fire is calculated using the well-known expression in Equation [3.14]:

$$\dot{Q} = \chi * \dot{m} * \Delta H_c \quad [3.14]$$

where  $\chi$  is the burning efficiency and  $\Delta H_c$  is the heat of combustion. It is very important that the heat of combustion and the burning efficiency in *Thimes* are the same as in the WPI/Fire Code, otherwise the HRR calculated in the WPI/Fire Code will be wrong.

Further changes that were made were: the Baroudi/Kokkala algorithm, which is a executable program, was turned into a subroutine called by the main program in the WPI/Fire Code and the mass loss rate was put in a table, together with the simulation time, serving as the only output from the *Thimes* subroutine. The flowchart in Figure 3.2 below displays the flame-spread code prior to and after the changes made.

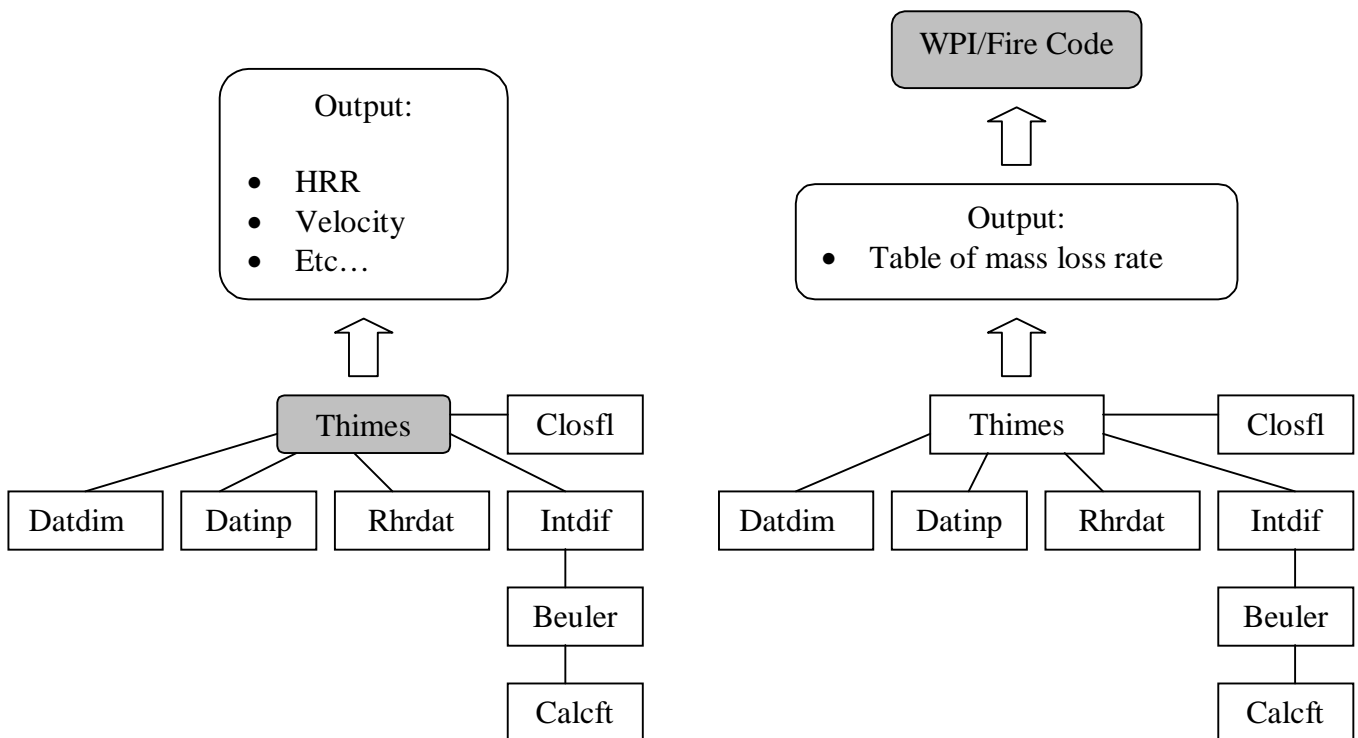


Figure 3.2. Flowcharts, showing the changes made in the flow of data.

To make sure that the integration of and the changes made to the flame-spread model did not effect the results of the calculations, the WPI/fire was executed using the same input data as the tests carried out by Baroudi et al. /Baroudi et al 1997/. The results presented in Appendix D, show that the correlation between the different results is very good. The small difference that occurs is due to that the HRR in WPI/Fire Code is calculated in a different way than by using Equation [3.14]. The difference is in the range of 1-2 percent for materials with a heat of combustion between 20 and 45 MJ/kg (most materials are within this range).

Some of the variable names have also been changed to fit the name system in the WPI/Fire Code. A list of this system can be seen in Appendix E.

## 4. THE WPI FIRE/CODE

This chapter contains a general introduction to zone models. Since the work that was carried out during this project involved the WPI/Fire Code, a deeper and more thorough explanation of this model will be made. Further, the changes made to the WPI/Fire Code will be described.

### 4.1 General on computer models

The use of computer models to simulate enclosure fires is a valuable tool when assessing the fire safety level in a building. Computer fire models can provide a faster and more accurate estimate of the impact of a fire than many of the methods previously used. While manual calculations provide good estimates of specific environmental factors caused by a fire, they are not well suited for comprehensive analyses involving the time dependent interactions of multiple physical and chemical processes present in developing fires. /Walton/

There are two major classes of computer models for analyzing enclosure fire development:

- ◆ *Stochastic or probabilistic* models generally treat fire growth as a series of sequential events or states. Mathematical rules are established to govern the transition from one event to another. Probabilities are assigned to each transfer point based on analysis of relevant experimental data, historical fire incident data and computer model results. /Walton/
- ◆ The *deterministic* models represent the processes encountered in a compartment fire by interrelated mathematical expressions based on physics and chemistry. The latest type of deterministic computer model is the *field model*. This type of model solves the fundamental equations of mass, momentum and energy for each element in an enclosure space that have been divided into a grid of smaller units. Due to the large amount of calculations these models are very time consuming. However, the most common type of deterministic models for simulating fires in enclosures is the *zone model*. /Walton/

### 4.2 General on zone models

The general form of a zone model is to divide each compartment into two zones, an upper layer which contains hot gases, and a cold lower layer which is often considered to be of ambient conditions. All parameters of each zone are homogeneous.

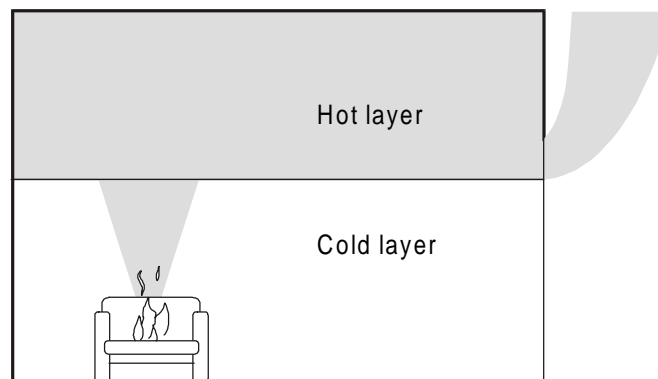


*Figure 4.1 Schematic view of a zone model. The compartment is divided into an upper, hot layer and a cold, lower layer. /Karlsson et al 1997/*

In both the control volumes (upper and lower layer) the state equations for energy and mass are solved simultaneously for small finite time steps, usually in the order of 0.1 seconds. The conditions in the room are determined for each time step. No zone-type fire model can provide an absolute answer, and each model has its limitations and errors. The physics of heat and mass transfer between each layer are not based on first principles. Rather, they are approximated with best-fit equations based on empirical fire tests. /Satterfield 1990/

The history of the zone-model codes started with simulation of fire in a single room with an open door for free ventilation. The open vent supplies air to the lower layer and then into the flame, which generates an upward exhaust gas stream, called the fire plume. The plume entrains air from the lower layer and gives the total mass input to the upper layer. Gas from the upper layer escapes to the nearby space through the free vent. Flow rates are given from mass preservation and pressure differences between the zones and the nearby space. Heat flows are given by heat release from combustion and heat flow by the plume to the upper layer. Convective heat flow is given between the upper layer and the ceiling. The ceiling, the upper layer, the fire plume and the flame transfer heat by radiation to walls and objects. Heat transferred through the ventilation is given by the ventilation flow.

### 4.3 Specific on the WPI/Fire Code

The WPI/Fire Code is a single room zone-type compartment fire model prepared at the Worcester Polytechnic Institute. It is based on the HARVARD fire model /Mitler 1979/ and the FIRST fire model /Mitler et al 1997/, but has additional physics options developed by Douglas Beller /Beller 1987/ and Peter Caffrey /Caffrey 1989/. Beller provides physics options for:

1. Calculation ceiling heat transfer based on the presence of a ceiling jet
2. Momentum driven mass flow through a ceiling vent.

Caffrey provides physics options for evaluating the formation of a hot spot on the wall or in a ceiling. /Barnett 1990/

#### 4.4 The WPI/Fire Code Fire Dynamics

The following section is a very brief summary of the physical model provided by the WPI/Fire Code.

In the WPI/Fire Code, a single room is modeled as having two gas layers, a cool lower layer at ambient conditions and a hot upper layer that forms from the fire plume.

The basic model is a deterministic and time dependent solution of simplified energy and mass conservation equations. The model also provides for formation of a fire plume over the burning object. It calculates heat transfer between the fire, other objects, walls and the ceiling. It provides for mass flow through multiple vents in the wall. It determines the environmental conditions in the room including layer temperatures and toxic gas species concentration.

Three types of burning objects may be simulated:

1. A fire growing on a horizontal surface of polyurethane.
2. A pool fire and
3. A liquid /gas fuel burner fire

All three types of burning object are limited by the oxygen available. An object may be initially non-burning, and ignited when the calculated surface temperature reaches a user-defined ignition temperature.

The fire plume above an object entrains air from the lower layer and carries it into the upper layer, due to buoyancy resulting in a hotter, less dense gas. The model provides for selection of one of six empirical fire plume models /Beyler 1986/:

1. Morton, Taylor, Turner
2. Same as above, but with point source
3. McCaffrey
4. Zukoski
5. Delichatsios/FM
6. Tokunga, Sakai, Kawagoe, Tanaka and Hasemi

Plume entrainment will also be changed by specifying whether the object is located away from all walls, against a wall or against a corner.

The upper layer is formed when the ceiling stops the gases of the fire plume. The basic program assumes, contrary to real fire dynamics, that the plume stops at the layer interface. Convective heat transfer to the upper walls and ceiling assume that the upper layer is still a mass of uniform temperature. This may under-predict the convective heat transfer in the early stage of hot layer formation. The selection of Beller's alternative physics routine for extended ceiling convective heat transfer accounts for the presence of a ceiling jet and increases the calculated convective heat transfer from the upper layer to the walls and the ceiling.

Wall vents are treated differently than ceiling vents. Wall vents allow for the natural outflow of hot gases and inflow of supply air, or both, depending on the position relative to the layer interface. Natural flow is driven by pressure differential and conservation of mass. By selecting Beller's ceiling vent physics option, a momentum-driven mass flow through a ceiling vent can be approximated. /Barnett 1990/

#### **4.5 Limitations of the WPI/Fire Code**

Barnett /Barnett 1990/ summarizes the following limitations for the WPI/Fire Code:

- Since the algorithms used in the WPI/Fire Code are empirically based, virtually every physical process modeled in the WPI/Fire Code has limits to their own applicability. There are no warnings when the model's errors become significant, giving unreasonable results.
- The WPI/Fire Code compartment models physics is not valid as the room approaches flashover or when the effect of the upper layer radiant heat flux become dominant. The WPI/Fire Code does not model ignition of the upper layer.
- Non-two-layer phenomena are not modeled. Neither is the stratification of gases before they reach the ceiling.
- The room must be vented. High-pressure effects on room dynamics and combustion are not considered.

#### **4.6 Adjustments for wall and corner plume in the plume sub-model**

Since the flame-spread model assumes that the burning occurs against a wall, an attempt was made to improve the plume model in the WPI/Fire Code. Some plume-models were compared to the experimental flame heights measured in the Baroudi/Kokkala experiments /Kokkala et al. 1997/. Delichatsios wall-plume with a line burner /Delichatsios 1984/ and Heskestads plume adjusted for the mirror effect /Karlsson et al. 1997/ showed best results. The Heskestad plume was chosen to be integrated into the WPI/Fire Code. Before the integration process, the algorithm was tested. The tests showed that the plume sub-model worked properly. However, when integrated, the Heskestad plume sub-model did not work as it should. The temperature of the upper layer remained constant. No further attempt to correct this error was made since this requires considerable programming skills and time effort. The source code to the plume model is shown in Appendix F.

Since the WPI/Fire Code has an option that allows the user to place a burning object against a wall or a corner, taking the mirror effect into account, it is still possible to model a single compartment fire with the flame-spread algorithm.

#### **4.7 Insertion of the Baroudi/Kokkala Algorithm into the WPI/Fire Code**

As mentioned in Chapter 3 several adjustments and changes in the Baroudi/Kokkala algorithm was necessary to be able to integrate it into the WPI/Fire Code. Further, some changes to the original WPI/Fire Code source code were also necessary. Several minor and major changes were therefore made. The most extensive addition to the WPI/Fire Code was a subroutine called WFIRE. WFIRE interpolates the correct mass-loss rate from the table (called ZASSA in the WPI/Fire Code ) created by the flame-spread algorithm at each given time-step. The changes and additions made to the WPI/Fire Code took considerable time due to the great size of the WPI/Fire source code and the authors modest skills in programming.



## 5. SENSITIVITY ANALYSIS ON INPUT PARAMETERS

In this chapter the scenario that was used to expose the input parameters to a sensitivity analysis will be explained. The exposed parameters will be listed. The results of the sensitivity analysis will be shown and finally some conclusions are drawn from the results.

### 5.1 Scenario

The scenario that this sensitivity analysis has been evaluated against consist of a 1.2 m wide and 2.4 m high wall made of porous fiberboard. A propane burner, 1.2 m wide and 0.2 high ignite the fiberboard. The burner's output is 100 kW. The flame height correlation factor,  $K$ , is set to  $6.5 \cdot 10^{-3} \text{ m}^2/\text{kW}$ . The time constant  $t_{ig}$  is taken as the time to ignition measured in the Cone calorimeter at an irradiance of  $25 \text{ kW/m}^2$  as the time when the HRR per unit area reaches  $50 \text{ kW/m}^2$ . The heat release data is taken from the cone calorimeter at an irradiance of  $25 \text{ kW/m}^2$ .

### 5.2 Variables included in the sensitivity analysis

To be able to see how the different input parameters to the flame-spread model affect the final result a simple sensitivity analysis was carried out. One parameter was varied, plus 50 % and minus 50 %, at the same time as the others where fixed. The plot named "original" is the test run with cone calorimeter data from  $25 \text{ kW/m}^2$  and with  $x_{p0}$  and  $K$  as given by Baroudi et al /Baroudi et al 1997/,  $0.2 \text{ m}$  and  $0.65 \cdot 10^{-5} \text{ m}^2/\text{W}$  respectively. Parameters analyzed are:

- Initial flame height,  $x_{p0}$
- Time to ignition,  $t_{ig}$
- Flame height correlation factor,  $K$

Further, an analysis of the influence from cone calorimeter data at different irradiance levels was carried out. This analysis includes:

- Combinations of cone calorimeter data, i.e. time to ignition and HRR per unit area, at  $25 \text{ kW/m}^2$  and  $50 \text{ kW/m}^2$

### 5.3 Results

The material tested in the sensitivity analysis is porous fiberboard on mineral wool. The result from this analysis is shown in Figures 5.1, 5.2, 5.3 and 5.4 below.

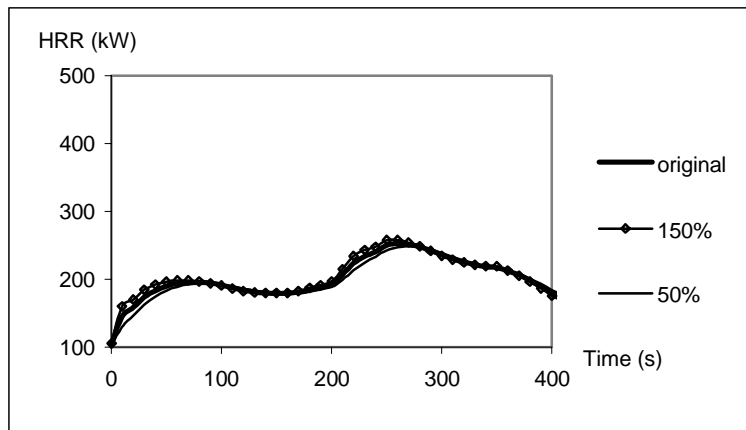


Figure 5.1 Sensitivity analysis on initial pyrolysis height,  $x_{p0}$

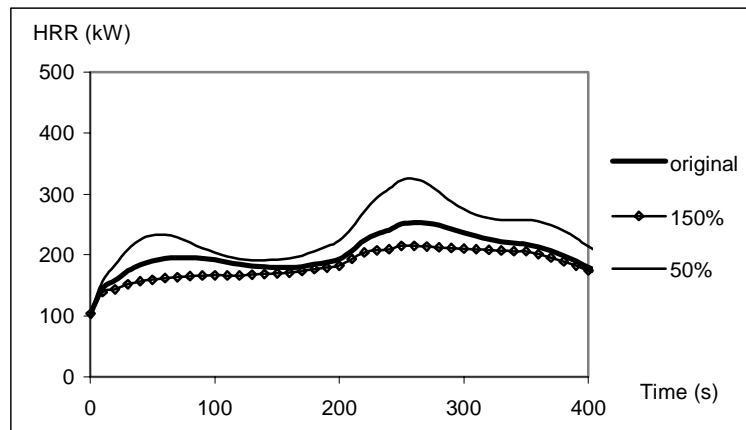


Figure 5.2 Sensitivity analysis on time to ignition,  $t_{ig}$

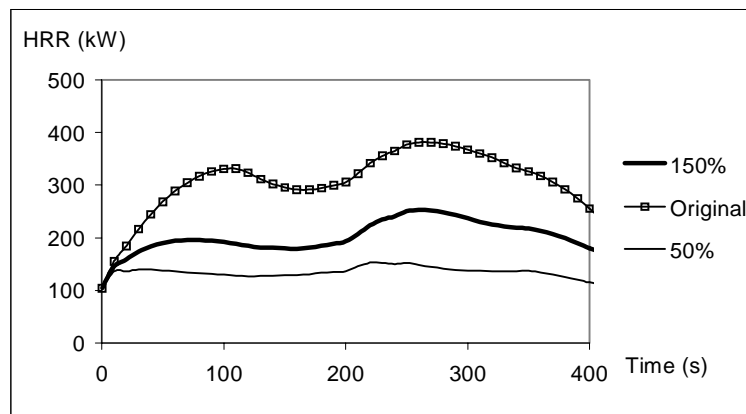


Figure 5.3 Sensitivity analysis on the flame height correlation factor,  $K$

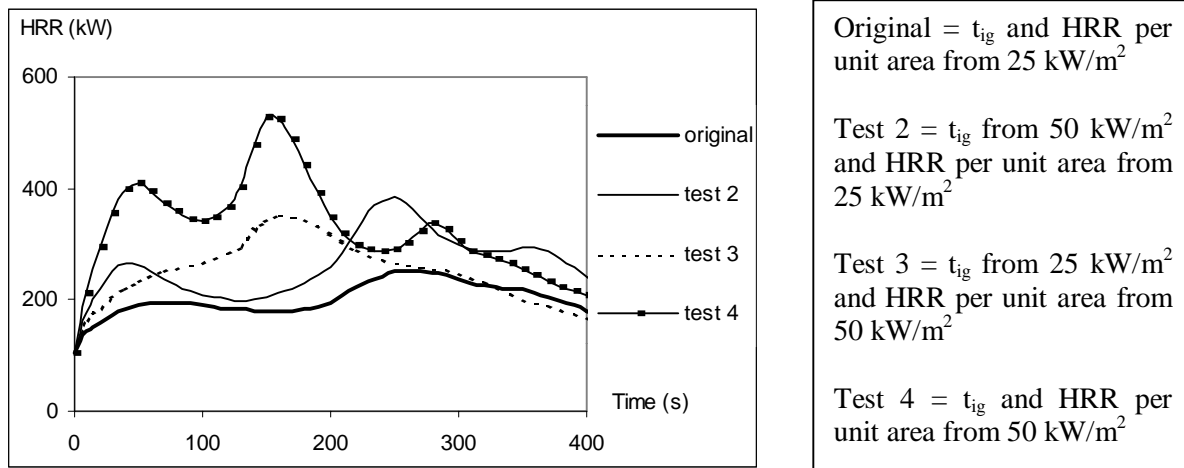


Figure 5.4 Cone calorimeter data combinations

## 5.4 Conclusions

1. Initial pyrolysis height, time to ignition and the flame height correlation factor all have a vertical effect on the result, i.e. the HRR peaks occur at the same time but with different magnitude.
2. Initial pyrolysis height has very little effect on the results while time to ignition and the flame height correlation factor have clear effects, flame length correlation factor being the most sensitive.
3. As expected the biggest difference is between the “Original” plot and “Test 4”. When using cone calorimeter data at 50 kW/m<sup>2</sup> the flame-spread is much faster and the peak HRR is also considerably higher. Looking at “Test 3” we can see that the peak HRR occurs earlier but the difference in magnitude is not that great. The last test, “Test 2”, gives a vertical change in HRR which is logical since it’s a further sensitivity analysis on time to ignition and therefore falls under the first conclusion.

Thus the most important parameters to look at are the flame height correlation factor and cone calorimeter data from either 25 or 50 kW/m<sup>2</sup>. The choice of cone calorimeter data depends on the end use condition, e.g. cone calorimeter data from 25 kW/m<sup>2</sup> is used for a wall fire while cone calorimeter data from 50 kW/m<sup>2</sup> might be more suitable for a corner scenario.

To summarize this, the parameters focused on when comparing simulated results and experimental results are:

- flame height correlation factor and
- cone calorimeter data, time to ignition and HRR, from either 25 or 50 kW/m<sup>2</sup>



## **6. TRANSLATION FROM BENCH SCALE TO FULL SCALE DATA**

This chapter explains the two models that is used when validating the code against experimental data. First in this chapter is a general discussion about translating bench scale data to full-scale data given. Further are the two models, Model A and Model B, described in detail. Finally, the two models are summarized.

### **6.1 General**

The growth of a fire in a room is highly dependent on the HRR from a burning material and the velocity of the flame-spread over it. In recent years mainly two types of methods have been proposed for prediction of these two. They are of various degrees of complexity and are used for different purposes. The two types of methods mentioned are:

1. One based on Computer Fluid Dynamics (CD) modeling with very sophisticated models for e.g. char depth, combustion and pyrolysis rate. These models are mainly used for testing and research purposes and product development. Still under development and no model generally available.
2. One based on so called thermal theories with rough assumptions on different parameters resulting in a computer model which is “fine tuned” against experimental data. Such models are mainly used for researchers, testing and design purposes.

There is also a difference in the amount of input data that is needed for the two models. The thermal theory models require less input data and are therefore easier to use. The bench scale tests that are often used for these models are the Cone Calorimeter and the Lateral Ignition and Flame-spread Test (LIFT) apparatus.

### **6.2 Modelling experiments in the WPI/Fire Code**

Since the flame-spread model used in this work is a thermal model the latter of the two ways to predict flame-spread and HRR is used, i.e. a computer model “fine tuned” against experiments. This is done in two steps, Model A and Model B. Both models are as mentioned based on the Baroudi/Kokkala flame-spread algorithm but with a few adjustments to fit the scenario which they are tested against.

### **6.3 Model A**

This model is tested against the experiments carried out by Baroudi/Kokkala when the algorithm was developed, i.e. a wall fire. The test configuration is shown in Figure 6.1 below. The tested material is attached to a 1.2 meter wide wall board on a vertical wood-framed sample holder. The backing of the board is either a 50 mm thick mineral wool or a 10 mm thick calcium silicate board. The propane burner's dimensions are  $1.2 \times 0.1 \times 0.1 \text{ m}^3$  and has an output of 40-300 kW. /Kokkala et al 1997/.

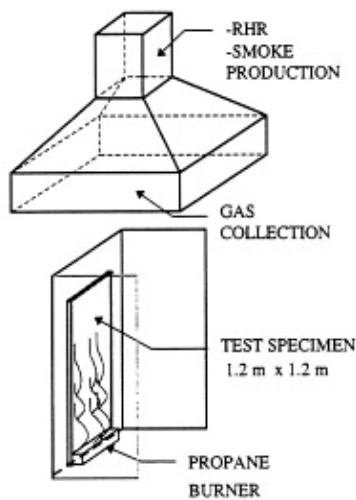


Figure 6.1 Test configuration, wall fire scenario /Kokkala et al 1997/

The purpose of Model A is to see if it is possible to get similar results with the WPI/Fire Code, using Cone Calorimeter data from  $50 \text{ kW/m}^2$  instead of  $25 \text{ kW/m}^2$ , compared to the results Baroudi/Kokkala got from their experiments. As shown in the sensitivity analysis, Chapter 5, the parameter to focus on, besides the Cone Calorimeter data, is the flame height correlation factor K. Thus when taking the time to ignition and HRR per unit area from  $50 \text{ kW/m}^2$  the K-value has to be changed, since the flame-spread otherwise becomes too fast.

When this scenario was simulated in the WPI/Fire Code, the following input data was used:

- Cone Calorimeter data from  $50 \text{ kW/m}^2$  and  $25 \text{ kW/m}^2$
- Initial pyrolysis height as 0.2 m (no change from the original value)
- The flame height correlation factor was changed to a value so the computational results would match the experimental data
- Time shift as the time to ignition in the Cone Calorimeter at  $50 \text{ kW/m}^2$  (no change from the original way)

To avoid influence of vitiation, the room in this scenario was modeled as a very large enclosure with large openings. The fire was fuel-controlled all the time.

## 6.4 Model B

Since one of the goals with this work is to incorporate a flame-spread model into a zone model, it is necessary to validate the model against experiments where the burning occurs in an enclosure. The most commonly used test of that kind is the ISO 9705 Room Corner Test. A schematic view of the test configuration is shown in Figure 6.2 below. The room measure  $2.4 \times 3.6 \times 2.4 \text{ m}^3$  with a door that measure  $2.0 \times 0.8 \text{ m}^2$  on a short wall. The tested material is mounted on the three walls opposite the doorway and on the ceiling if desired. A  $0.17 \times 0.17 \text{ m}^2$  propane burner is located in a corner, in contact with both walls /Dillon et al 1998/. The materials tested in this model are apart of either the Swedish materials /Karlsson 1992/ or the Eurefic materials /Wickström 1993/.

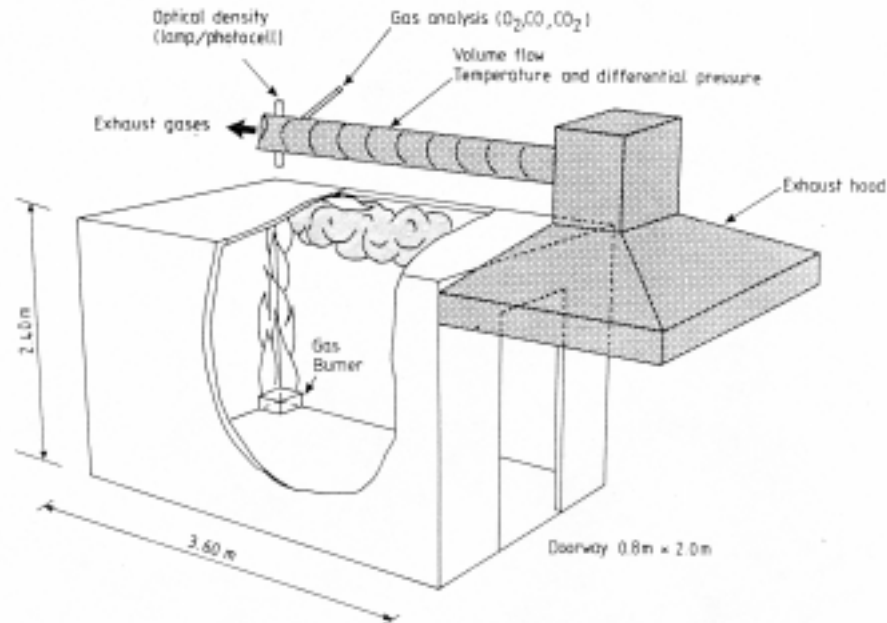


Figure 6.2 Test configuration, ISO 9705 Room Corner scenario /Sundström 1990/

As the flame-spread model is based on a wall fire and the experiment that Model B is tested against is a corner scenario, some further changes have to be made. The sensitivity analysis states that Cone Calorimeter data from  $50 \text{ kW/m}^2$  might be more suitable for a corner scenario than data from  $25 \text{ kW/m}^2$ , therefore is Cone Calorimeter data from  $50 \text{ kW/m}^2$  also used in this model. In accordance with Model B the K-value will be changed to fit the corner scenario.

In /Baroudi et al 1997/ the author mentions that the heat flux behind a  $100 \text{ kW}$  burner is in the range of  $20 - 45 \text{ kW/m}^2$ , depending on the height above the surface. This states that a time shift based on Cone Calorimeter data from  $50 \text{ kW/m}^2$  might be too short. The results from the tests in /Baroudi et al 1997/ also indicates this. So, in Model B, the time shift will be taken from Cone Calorimeter data at a lower irradiance level.

The final change made to the flame-spread model is the burner width. The burner in the ISO 9705 test is a square burner in the corner and therefore it has two sides against a wall. The width of this burner is  $0.17 \text{ m}$ . Looking at the corner as a folded wall and giving the simulated burner width the value of about two square burners solves this. The proceeding of Model B can now be summarized as:

- Cone Calorimeter data from  $50 \text{ kW/m}^2$
- Initial pyrolysis height as  $0.2 \text{ m}$  (no change from original value)
- The flame height correlation factor was changed to a value so the computational results would match the experimental data
- Burner width is approximated to  $0.3 \text{ m}$  ( $0.17 \text{ m} + 0.17 \text{ m}$ )
- Time shift as time to ignition at a lower irradiance level than  $50 \text{ kW/m}^2$

After a few rounds of trail and error the best fit was achieved when the flame height correlation factor was set to  $0.15 \cdot 10^{-4} \text{ m}^2/\text{W}$ . This is within the range given by Karlsson /Karlsson 1992/, and the time shift as the time to ignition at  $35 \text{ kW/m}^2$ .

## 6.5 Summary

Two different models are used when evaluating the code against experiments. Model A compare data from a free burning wall with data calculated by the WPI/Fire Code. In this case is cone calorimeter data at an irradiance level of  $50 \text{ kW/m}^2$  used instead of data at an irradiance level of  $25 \text{ kW/m}^2$ . The parameter to focus on in this model is the flame height correlation factor, K. The cone data at the higher irradiance level will increase the flame spread velocity. The K-value has to be lowered to keep the velocity at a lower level.

Since the WPI/Fire Code is a zone model, evaluation has to be made against an enclosure. Model B compares data from the ISO 9705 Room Corner Test with data calculated by the WPI/Fire Code.

## 7. COMPARISON WITH EXPERIMENTAL DATA

In this chapter the results from the evaluation process will be presented. An evaluation of the WPI/Fire Code against experiment was necessary after the flame-spread model had been integrated into the WPI/Fire Code. As mentioned earlier in Chapter 5 two models, Model A and Model B, were used for evaluation. Model A was the first one to be evaluated.

### 7.1 Evaluation of Model A

As described in Chapter 5, Model A uses as input cone data at irradiance levels of  $25 \text{ kW/m}^2$  and  $50 \text{ kW/m}^2$  when comparing to experiments. The results show that the flame-spread velocity becomes too fast when calculated with  $50 \text{ kW/m}^2$  data. One way of lowering the flame-spread velocity is to lower the flame height correlation factor. However, when the flame height correlation factor was lowered to the level where the HRR showed reasonable comparison with  $25 \text{ kW/m}^2$  data, the value of the correlation factor became unrealistically low. The value of the correlation factor became as low as  $0.35 \cdot 10^{-5} \text{ m}^2/\text{W}$ . Some examples are given in Figures 7.1-7.2. The figures show results from calculations with different value on the flame height correlation factor.

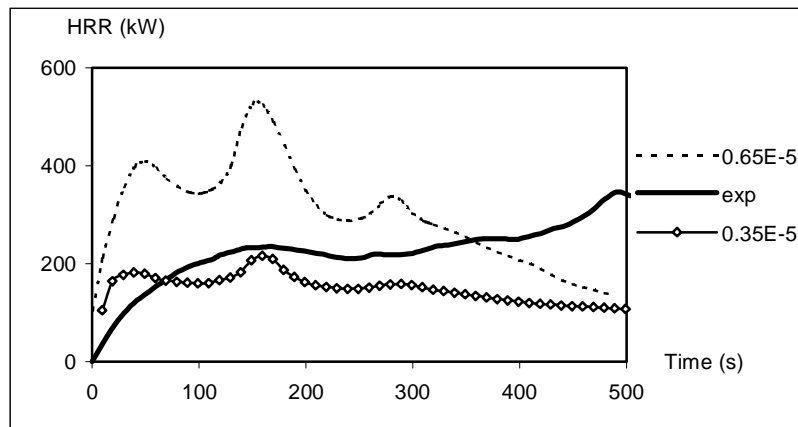


Figure 7.1. Porous fibre board on mineral wool

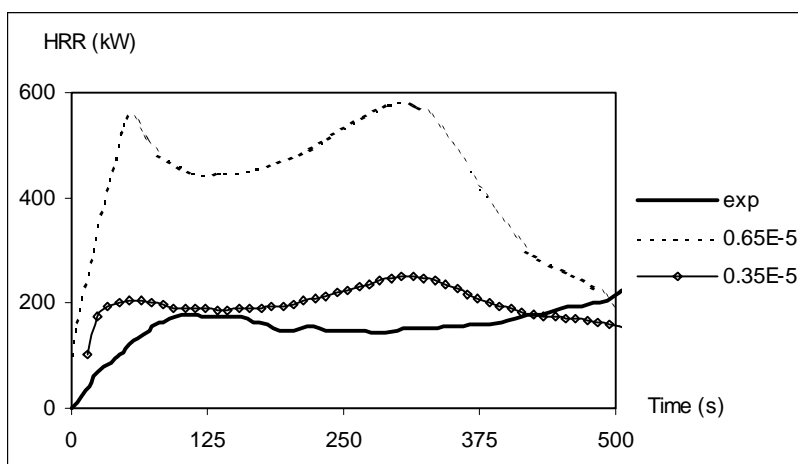


Figure 7.2. Wood (moist)

All the results from the materials tested with Model A are shown in Appendix G.

## 7.2 Evaluation of Model B

Since the results from the evaluation of Model A became unrealistic, Model B had to be tested as well. Model B is described in Chapter 5 and compares data from the ISO 9705 Room Corner Test with the output data from the WPI/Fire Code. The main output parameter that the code was validated against was of course the HRR, but the gas temperature was also compared since the temperature parameter is of great concern for the user when using a zone model.

When comparing the HRR, almost all the tested materials showed very good comparison with experiments, results in Appendix H. Plastic based materials did not show as good results as the wood based materials, Figure 7.2, 7.3 and 7.4.

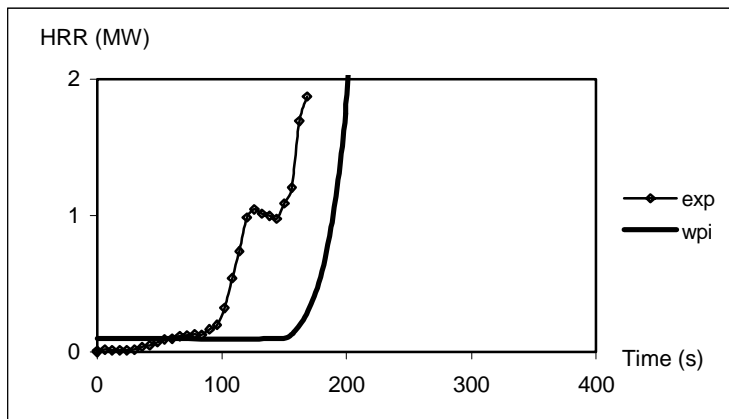


Figure 7.2 Expanded polystyrene. A plastic based material

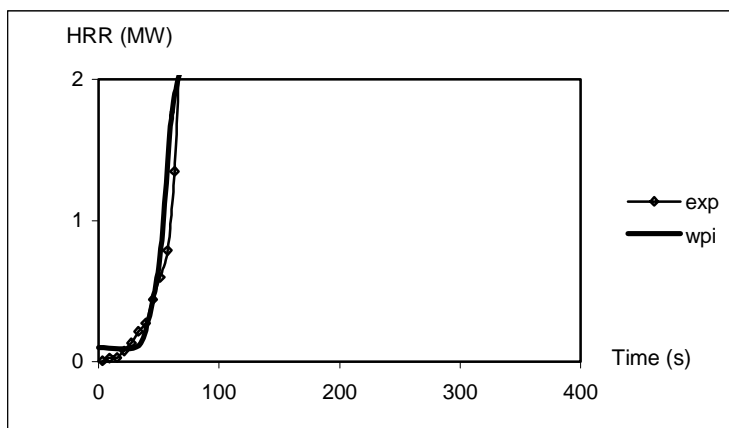


Figure 7.3 Insulating fibreboard. A wood based material

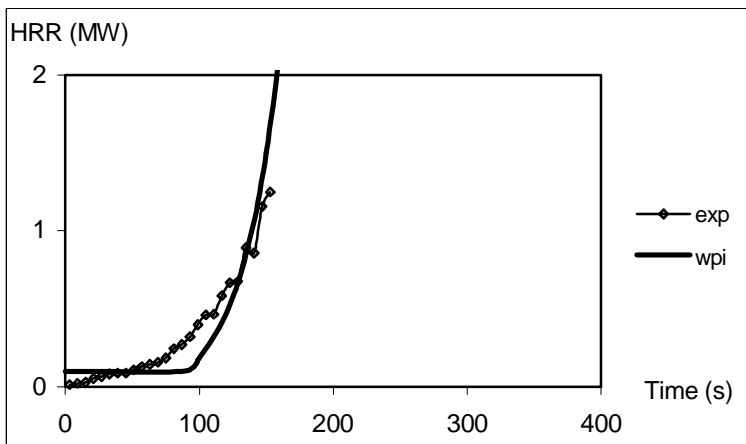


Figure 7.4. Paper wall covering on particleboard. A wood based material

Common for all materials is that the gas-temperature calculated with the WPI/Fire Code is lower than the measured temperature in the ISO 9705 test, see Figure 7.5-7.6.

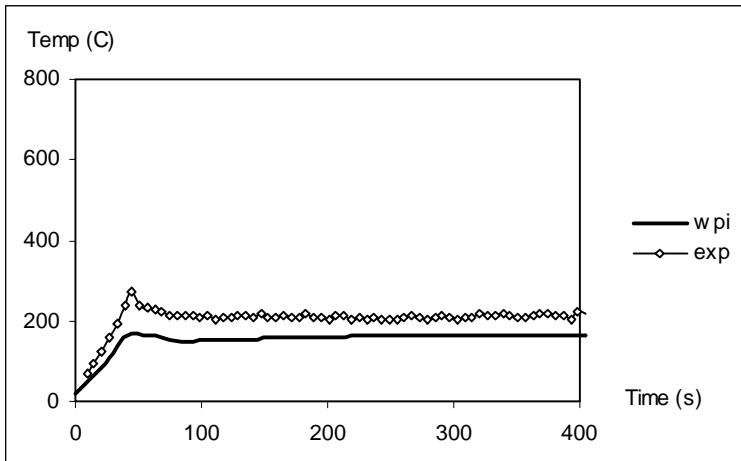


Figure 7.5. Plastic wall covering on gypsum board.

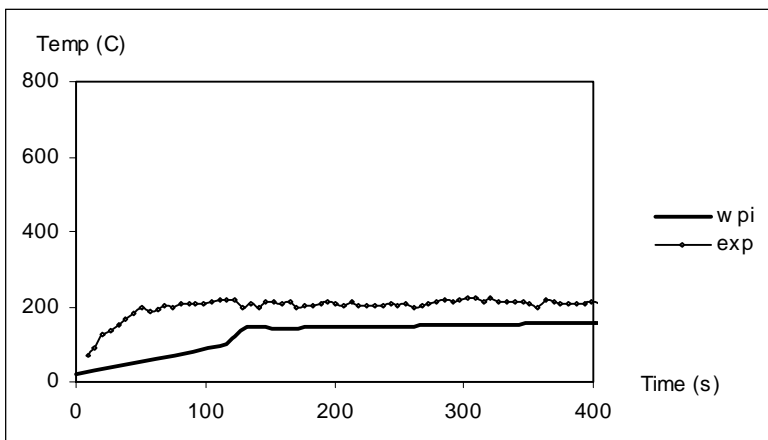


Figure 7.6. Gypsum board

One possible reason for this phenomenon is that the plume model calculates a mass-loss rate that is higher than mass-loss rate in the ISO 9705 test. The upper layer thickness becomes greater when calculated with the WPI/Fire Code and the energy from the plume become divided on a larger volume. This leads to a lower gas temperature. This might be achieved if a proper wall plume is added to the source code.

Another reflection from the tests is that the time when 1 MW is reached is roughly the same time when 300 °C is reached. As mentioned in Chapter 1, 300 °C is the temperature when the flame-spread model is not valid anymore. Thus, our limitation coincides with the theoretical HRR limit for flashover in the ISO 9705 test (1 MW) /Karlsson et al 1997/. The result of this could be that the WPI/Fire Code could be used as a tool when evaluating a new materials behavior in the ISO 9705 test.

When simulating materials that reach flashover, the height of the wall ( $Y_{max}$ ) had to be increased to a higher value. In the ISO 9705 test the ceiling ignites as well for these kinds of materials. The flame-spread model assumes a free burning wall without a ceiling. To correct this the 3-dimensional wall/ceiling configuration is modeled only as a 2-dimensional wall. Karlsson /Karlsson 1992/ solved the flame-spread under the ceiling as a function of area and there is no difference which geometry the area has. So the ¼-circular flame-spread that takes place under the ceiling can be modeled as a rectangle. This justifies our choice to increase the  $Y_{max}$  value.

### 7.3 Summary

The flame-spread algorithm uses cone calorimeter data as input. When cone data at an irradiance level of 50 kW/m<sup>2</sup> was used in Model A, the flame-spread became too fast. To compensate for this increase in flame-spread velocity was the flame height correlation factor lowered. However, the flame height correlation factor had to be lowered to an unreasonable low value if the calculated data would match the experimental data.

When cone data at an irradiance level of 50 kW/m<sup>2</sup> was used in Model B, the results from the calculations of the HRR showed good agreement with the experimental data, especially for the wood based materials. The flame height correlation factor had a value within reasonable limits.

The WPI/Fire Code generally underestimated the upper layer temperature. This phenomenon can be explained by the plume-model. If the plume-model overestimates the mass-loss rate, the upper layer temperature will be lower.

The evaluation of Model B also shows that 300 °C is reached roughly at the same time as the theoretical maximum HRR in the ISO 9705 room is reached.

## **8. CONCLUSION AND RECOMMENDATIONS ON FURTHER WORK**

The main goal of the project was to integrate a flame-spread algorithm into a zone model. The Karlsson model /Karlsson 1992/ as presented by the Baroudi/Kokkala algorithm /Baroudi et al/ was chosen as the flame spread model and the WPI/Fire Code was chosen as the zone model. Even though the WPI/Fire Code is able to calculate HRR from flame-spread correctly it is not correct to say that the flame-spread model is fully integrated into the WPI/Fire Code. A complete integration would be that the mass-loss rate from flame-spread is calculated at each time step and not for the whole simulation period and then interpolated for the correct time step, as the result of this project is. A complete integration requires more programming skills than the authors possess. However, the results of the simulations will be the same, irrespective of the sophistication of the integration.

A more correct integration and some further work on the wall plume as well as verifying against some more materials and scenarios would make an interesting senior project in the future.



---

## REFERENCES

- Babrauskas, V. Twilley, W. User's Guide for the Cone Calorimeter. National Bureau of Standards, U.S. Department of Commerce. August 1988.
- Barnett, Jonathan B., Satterfield, David B. User's guide to WPI/HARVARD Version 2. Center for Firesafety Studies, Worcester Polytechnic Institute. August 1990
- Baroudi, D. Kokkala, M. Parker, W. THIMES a computer program for upward flame calculations. Technical Research Centre of Finland (VTT).
- Baroudi, D. Kokkala, M. Parker, W. Upward Flame Spread on Wooden Surface Products: Experiments and Numerical Modelling. Technical Research Centre of Finland (VTT). 1997
- Beller, D K. Alternate Computer Models of Fire Convection Phenomena for the Harvard Computer Fire Code. Worcester Polytechnic Institute. 1987
- Beyler, C.L. Fire Plumes and Ceiling jets. Fire Safety Journal 11, 1986.
- Caffrey, P. J. Computer Modelling of Hot Spot Formation on Walls Using Non-Ventilated Heat Transfer Phenomenon. Worcester Polytechnic Institute. 1989
- Carslaw, H. S. Jaeger, J.C. Conduction of Heat in Solids, Oxford University, Oxford, 1959
- Dahlberg, Martin. The SP Industry Calorimeter for Rate of Heat Release Measurements Up to 10 MW. Swedish National Testing Institute. 1992
- Delichatsios, M. Flame Heights in Turbulent Wall Fires with Significant Flame Radiation. Fire Science and Technology 1984 vol 39.
- Dillon, Scott Edward. Analysis of the ISO 9705 Room/Corner Test: Simulations, Correlations and Heat Flux Measurements. University of Maryland. August 1998
- Edward, C.H. Penney, D. E. Calculus & Analytic Geometry, 2<sup>nd</sup> Edition. 1956.
- Janssens, Marc L. Measuring Rate of Heat Release by Oxygen Consumption. Fire Technology Volume 27 Number 3. August 1991
- Karlsson, Björn. Modeling Fire Growth on combustible lining materials in enclosures. Department of Fire Safety Engineering, Lund University. 1992
- Karlsson Björn, Thomas Philip H. On Upward Flame Spread on Thick Fuels. Department of Fire Safety Engineering, Lund University. December 1990.

Karlsson, B. Quintiere, J G. Enclosure Fire Dynamics, A first Draft of a Student Textbook. Department of Fire Safety Engineering, Lund University. August 1997

Kokkala, M. Mikkola, E. Immonen, M. Juutilainen, H. Manner, P. Parker, W. Large-scale Upward Flame Spread Test on Wood Products. Technical Research Centre of Finland (VTT). 1997

Mitler, H E. User's Guide for the Harvard Computer Fire Code. Harvard University, Division of Applied Sciences. 1979

Mitler H E, Rockett J A. User's Guide to FIRST - A Comprehensive Single-Room Fire Model. U S Dept of Commerce - Nat Bureau of Standards NBS. 1987

Satterfield, David B. Documentation for the WPI/HARVARD version 2 computer model. Worcester Polytechnic Institute. August 1990

Sundström, Björn. A New Generation of Large Scale Test Methods. Swedish National Testing Institute. 1990

Walton, W.D. Zone Computer Fire Models for Enclosures. The SFPE Handbook of Fire Protection Engineering, 2<sup>nd</sup> Edition.

Wickström, Ulf. Summary Report of the EUREFIC Programme. Swedish National Testing Institute. 1993

**APPENDIX A. TIME TO IGNITION AND EXTERNAL HEAT FLUX**

This Appendix contains the  $t_{ig}$  [s] vs.  $\dot{q}_{ext}''$  [kW/m<sup>2</sup>] plots for the Eurefic materials. The plots were used to determine the maximum external heat flux allowed.

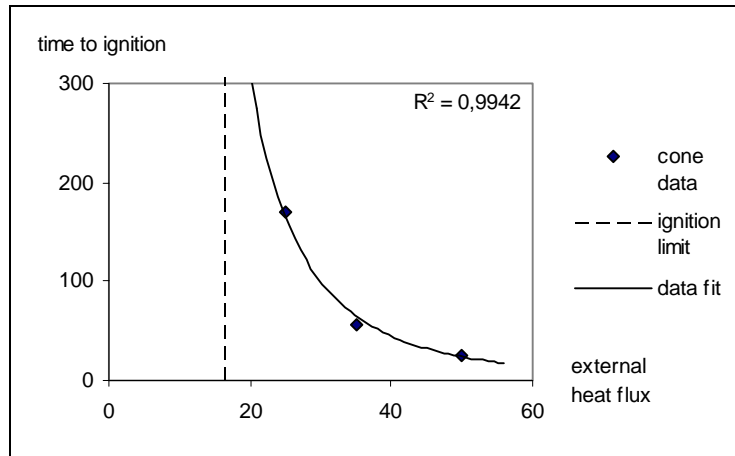


Figure A1. Ordinary plywood, E2

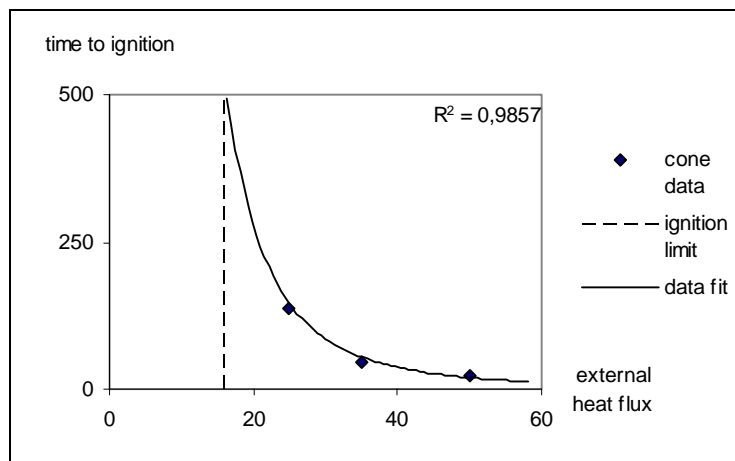


Figure A2. Textile wall covering on gypsum paper plaster board, E3

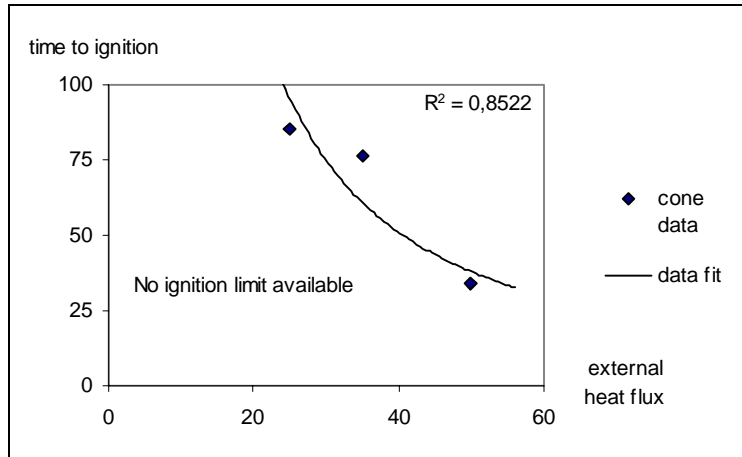


Figure A3. Plastic faced steel sheet on mineral wool, E5

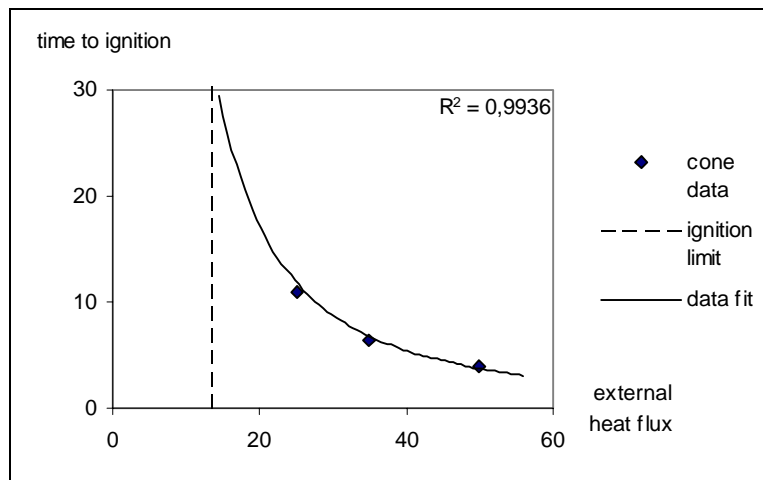


Figure A4. Faced rockwool, E7

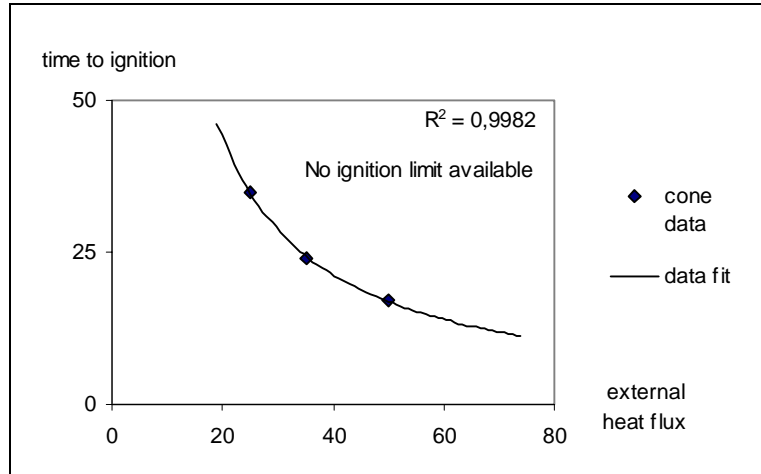


Figure A5. PUR foam covered with steel sheet, E9

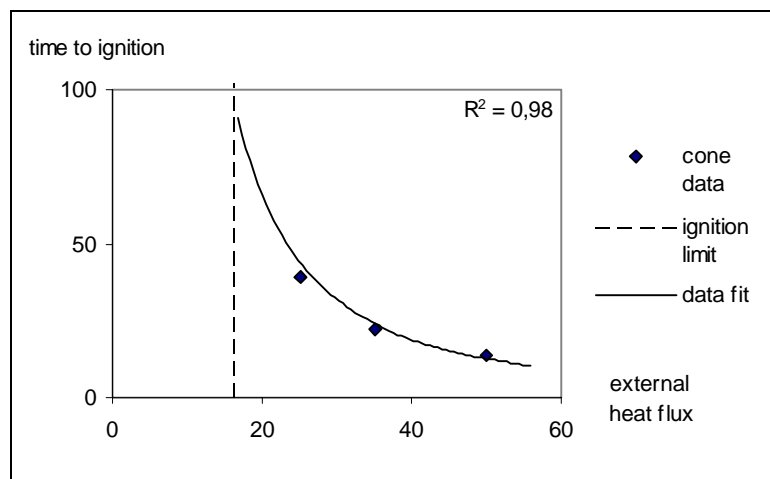


Figure A6. PVC wall carpet on gypsum paper plaster, E10



## APPENDIX B. INFLUENCE OF EXTERNAL HEAT FLUX

This appendix contains the percentage difference plots for the Eufic materials used to determine the maximum external heat flux allowed. The percentage difference limit is set to 10 %, which is shown in the plots.

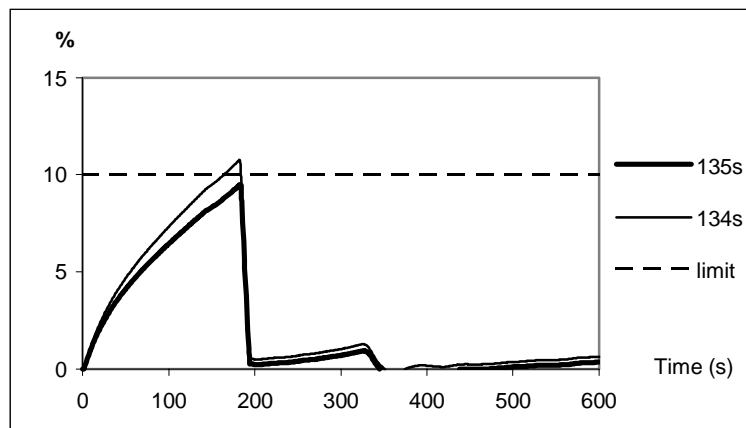


Figure B1. Ordinary plywood, E2

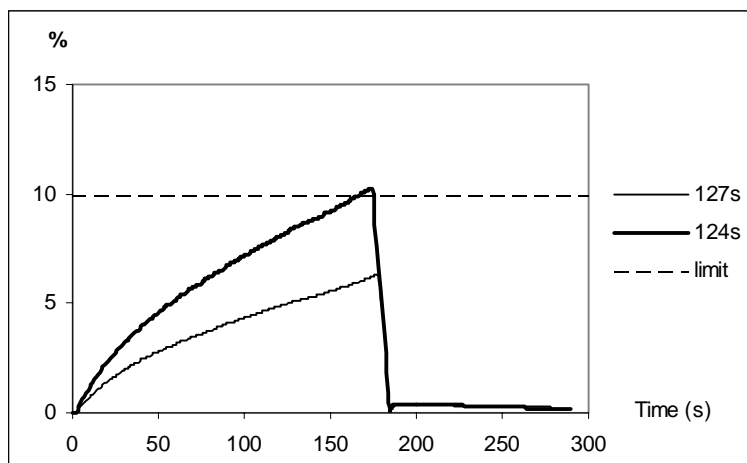


Figure B2. Textile wall covering on gypsum paper plaster board, E3

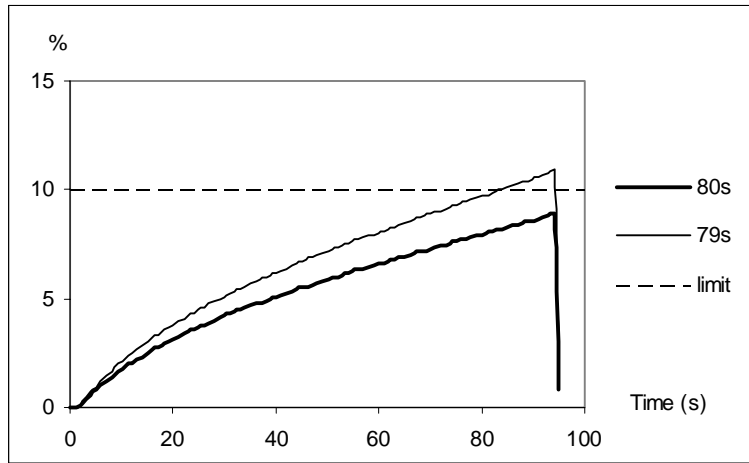


Figure B3. Plastic faced steel sheet on mineral wool, E5

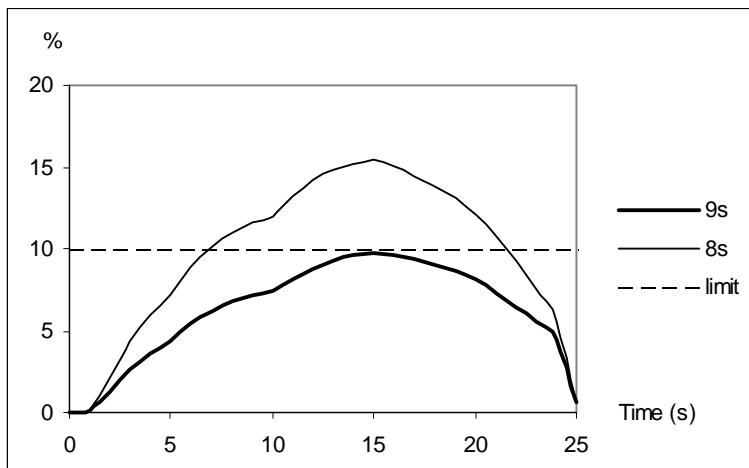


Figure B4. Faced rockwool, E7

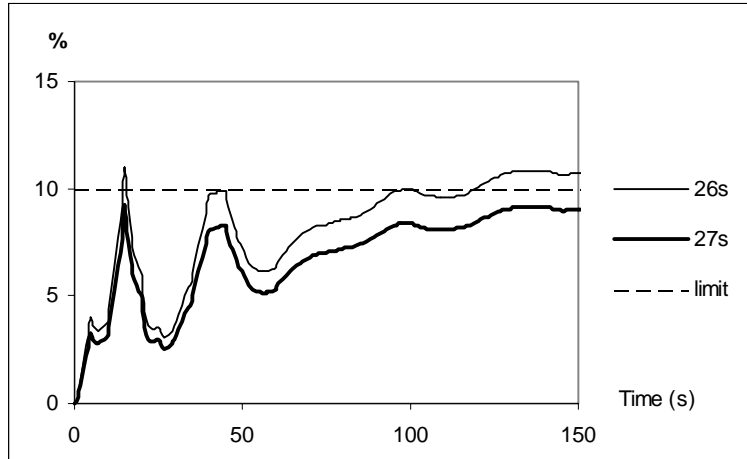


Figure B5. PUR foam covered with steel sheet, E9

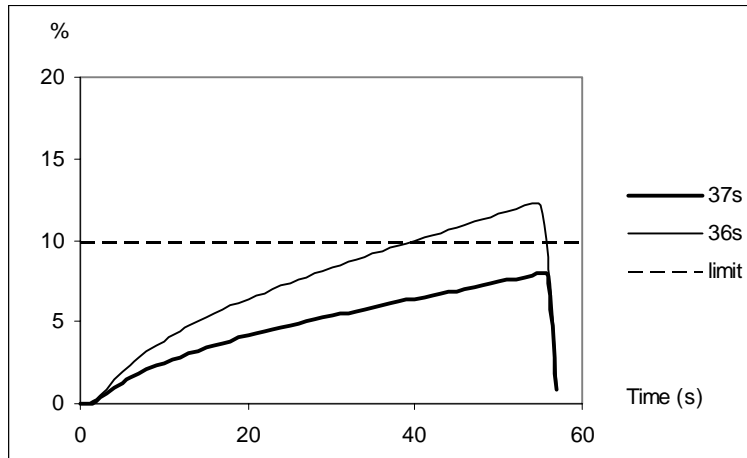


Figure B6. PVC wall carpet on gypsum paper plaster board, E10



**APPENDIX C. INPUT DATA FILE TO *THIMES***

This Appendix shows how input data files to *Thimes* would look like. The first row consists of dummy variables. These should not be changed. The second, third and fourth rows consists of material properties and some constants that relate to the flame spread algorithm. Finally is cone data presented in two columns, in the left column is the time (after ignition) presented and in the right column is the heat flux per unit area presented.

```

1      13      10
NDIM   NPROP   NPRINT

1  0  .2  .65E-5  37  0.  1.2  83.33E3  1  50.E3  20.0E6  41.7E6  0.65
n  x0  xp0    K    τig  τ0  Wburner  Qb    α    qcone,0  ΔHc,wall  ΔHc,burner  χ

1.      0.  1200.
Δt      τmin  τmax

.2      2.4
Y0      Ymax

RHR-curve  [W/m2]:
0          50000
5          117000
10         137000
15         124000
20         115000
25         124000
30         114000
35         106000
40         102000
45         95000
50         90000
55         86000
60         82000
65         78000
70         75000
75         73000
80         71000
85         70000
90         68000
95         66000
100        66000
120        61000
140        69000
160        70000
180        83000
200        88000
220        137000
240        104000
250        112000
300        74000
350        80000
500        0

```



## APPENDIX D. COMPARISON OF RESULTS

These are the plots showing the results from the comparison between the HRR calculated by *Thimes* and the HRR calculated by the WPI/Fire Code. The plots are almost identical, which shows that the integration process was successful.

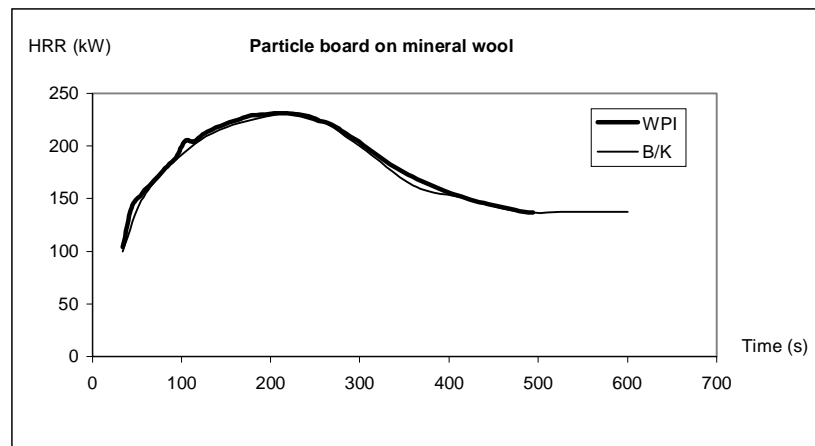


Figure D1. Particle board on mineral wool

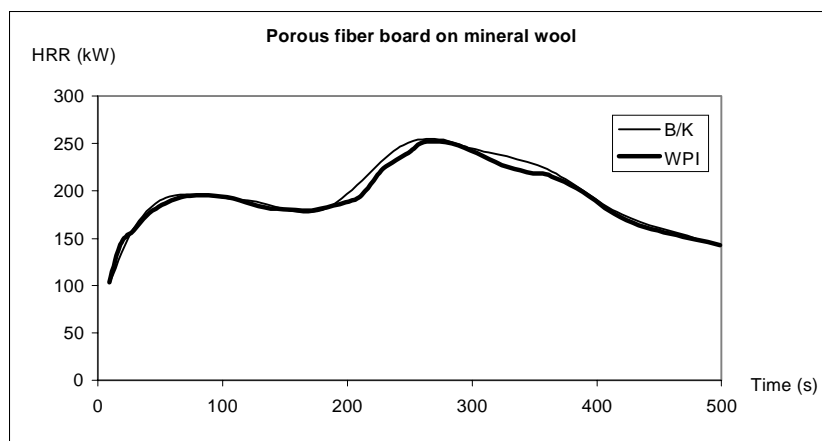


Figure D2. Porous fiber board on mineral wool

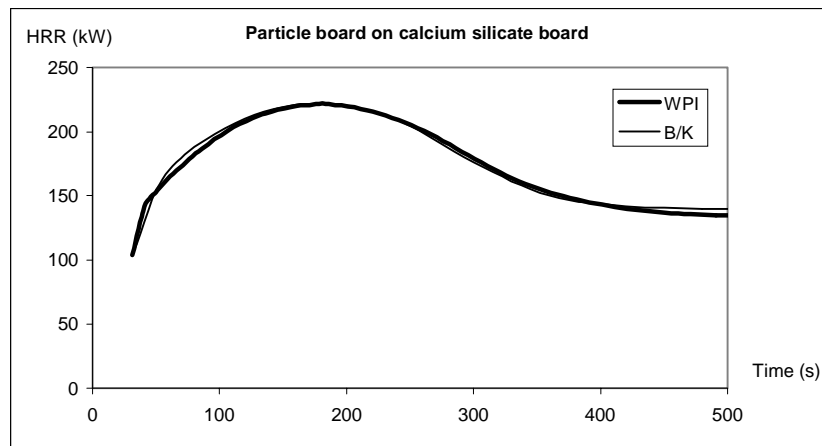


Figure D3. Particle board on calcium silicate board

## APPENDIX E. NOMENCLATURE IN THE WPI/FIRE CODE

Since there is a large number of geometrical and physical properties involved in an enclosure fire special measures must be taken not to mix up all the variables. Two variables cannot be assigned the same name.

In the WPI/fire code each variable has a name that consist of 6 characters. Each character has a pre-assigned purpose. The following section is taken from /Satterfield 1990/.

- The first character is used for derivates, with respect to:

Z	nothing
T	Time
X,Y,Z	Space
A	Area
V	Volume
F	Area and time
S	Space and time
D	Difference delta, exact definition to be specified by the user.

- The second character is used for physical quantity:

A	Area	N	Thickness
B	Width	O	Heat transfer coefficient
C	Specific heat	P	Pressure
D	Diffusion coefficient	Q	Heat transferred
E	Energy	R	Emissivity, Radius
F	View factor	S	Coordinate
G	Thermal diffusivity	T	Time
H	Height	U	Absorptivity
I	Radiant intensity	V	Volume
J	Thermal conductivity	W	z-coordinate
K	Temperature	X	Mole fraction, x
L	Length	Y	Mole fraction, y
M	Mass	Z	Nothing, z-coordinate

- Position 3 and 4 specifies an object, place or direction; e.g. position3 (from) and position 4 (to):

A	Ambient	R	Room
C	Cool (lower) layer	U	Upper (as in "above")
D	Down (as in below)	V	Vent
F	Fuel	W	z-direction, or wall.

L	Hot (upper) layer	Y	y-direction
O	Object (will include all objects, distinguished by subscripts)	Z	Nothing
P	Plume		

- Position 4 specifies a composition variable:

B	Charring plastics	J	Char
C	Cellulose	M	Carbon monoxide
D	Carbon dioxide	N	Nitrogen
E	Soot	O	Oxygen
G	(or HC) combustible gas or hydrocarbon.	P	Plastic
H	Hydrogen	S	Smoke
I	Inert ingredients	W	Water (H <sub>2</sub> O vapour)
		Z	Zone

- Position 5 specifies special conditions:

A	Ambient	I	Initial condition
B	Boundary conditions	M	Maximum Value
C	Critical conditions	N	Minimum value
D	Convection	R	Radiation
E	Outside	S	Sum
F	Final condition	Z	None

- Position 6 is normally left blank. However, it is used as a suffix for numerical handling:

0	(zero) or P – Value at previous time step.
1	Value on output from the current physical subroutine.

Examples:

ZKLZZ  
123456

- The Z in the first position means that there are no derivatives.
- The K in the second position stands for temperature.
- The third position gives us a location, in this case it is an L that stands for the upper layer.
- The fourth and fifth positions consists of Z. Z usually means “nothing” so in this case they do not fill any purpose.

Since the only positions that actually mean anything are number 2 and 3, which stand for temperature and upper layer, *the variable ZKLZZ stands for the temperature in the upper layer.*

**APPENDIX F. THE SOURCE CODE TO THE SUBROUTINE *WPLUM***

This Appendix contains the source code *WPLUM* that is based on the Heskestad plume model. The code is written in FORTRAN.

```

C*****
C
C   SUBROUTINE WPLUM(ZRFZZ,TMOZZ,CHI,QF,ZHPZZ,VMAZZ,ZKAZZ,TMPZZ1)
C
C*****
C   This subroutine calculates the massflow at the top of the
C   plume into the hot upper layer. It is based on Heskestads
C   plume equations (SFPE Handbook, section 2 chapter 2) using
C   the mirror effect, i.e 1/2 the massflow for plume in center
C   of room with twice the heat release rate and twice the area
C   of fire. Added 25 juli 1998.
C
C   Programmer: Gojkovic, D and Hultquist, H
C
C   Referense:
C
C   These are the main variables and constants:
C
C   Constants
C   CP = SPECIFIC HEAT OF AIR = 1004
C   BIGE = CONSTANT IN PLUME EQUATION = 0.196
C   G = ACCELERATION DUE TO GRAVITY = 9.81
C   BIGG = CONSTANT IN PLUME EQUATION = 2.9
C   PI = 3.1415927
C
C   Variables
C   ZDFZZ = EQVIVALENT DIAMETER OF BURNER
C   ZLFZZ = FLAME HIGHT
C   TMPZZ = MASS FLOW OUT OF THE TOP OF THE PLUME
C   TMPZZ1 = MASS LOSS RATE OF OBJECT INCLUDED
C   TEOZZ = HEAT RELEASE RATE FROM OBJECT
C   ECONV = CONVECTIVE PART OF TEOZZ
C   VMDZZ = DENSITY OF LOWER LAYER
C   ZKDZZ = TEMERATURE OF LOWER LAYER
C   VMAZZ = DENSITY OF AMBIENT AIR = 1.177 AT 300 K
C   ZKAZZ = TEMERATURE OF AMBIENT AIR = 300 K
C   VORIG = VIRTUAL ORIGIN OF FIRE
C   ZHPZZ = HIGHT OF PLUME, FROM BASE OF FIRE UP
C           TO THE INTERFACE
C   QF = HEAT OF COMBUSTION OF OBJECT
C

```

```

C  Recall that TEOZZ is a negative number!
c
C  Assigning values for constants:
C
  IMPLICIT DOUBLE PRECISION (A-H,O-Z)
  PARAMETER (BIGE=0.196D0, BIGG=2.9D0)
  PARAMETER (G=9.81D0, CP=1004.D0)
  PARAMETER (PI=3.1415927D0)

C  Calculates equivalent diameter of fire:
  ZDFZZ = SQRT(2.D0*4.D0*ZRFZZ*ZRFZZ)
C
  TEOZZ = TMOZZ*CHI*QF/1000.D0
C
C  Calculates flame hight:
  ZLFZZ = 0.235D0*(-TEOZZ*2.D0)**(2.D0/5.D0)-1.02D0*ZDFZZ
C
C  Calculates virtual origin:
  VORIG = 0.083D0*(-TEOZZ*2.D0)**(2.D0/5.D0)-1.02D0*ZDFZZ
C
  TMPZZ1 = -TMOZZ
  IF (ZHPZZ .LT. 0.D0) GO TO 15
  IF (TEOZZ .GE. 0.D0) GO TO 15
C
C  Determines if (ZHPZZ > ZLFZZ), (ZHPZZ < ZLFZZ) or (ZHPZZ=ZLFZZ)
C  and calculates the massflow there after:
C
  IF (ZHPZZ .GT. ZLFZZ) THEN
c    Interface above flamehight
C
C  Uses zkazz and vmazz as temperatur and density of lower layer
C
  T1 = 0.5D0*BIGE*(G*VMAZZ*VMAZZ/CP/ZKAZZ)**(1.D0/3.D0)
C
  T2 = BIGG*(SQRT(G)*CP*VMAZZ*ZKAZZ)**(-2.D0/3.D0)
C
  TMPZZ = T1*(-TEOZZ*0.7D0*2.D0)**(1.D0/3.D0)*(ZHPZZ-VORIG)**
1(5.D0/3.D0)*(1.0D0+T2*(-TEOZZ*0.7D0*2.0D0)**(2.D0/3.D0)*
1(ZHPZZ-VORIG)**(-5.D0/3.D0))
C
  ELSE
    IF (ZHPZZ .LT. ZLFZZ) THEN
C    Interface below flamehigh
c
  TMPZZ = 0.5D0*0.0056D0*(-TEOZZ*2.D0*0.7D0)*ZHPZZ/ZLFZZ
C

```

```
      ELSE
C     Interface at flamehight
C
      TMPZZ = 0.5D0*0.0056D0*(-TEOZZ*2.D0*0.7D0)
C
      END IF
      END IF
C
C SAFETY AGAINST BAD FLUCTUATIONS
C
      IF(TMPZZ .LE. 0.D0) GO TO 15
C
      TMPZZ1 = TMPZZ - TMOZZ
C
      15 CONTINUE
C
C CHECK MAGNITUDE OF OUTPUT VARIABLES
C
      IF (TMPZZ1 .LT. 0.D0) TMPZZ1 = 0.D0
      IF (TMPZZ1 .GT. 1000.D0) TMPZZ1 = 1000.D0
c
      RETURN
      END SUBROUTINE
```



## APPENDIX G. MODEL A

This appendix shows the results from the evaluation of Model A. The different lines in the graphs shows experimental results and calculations with different flame height correlation values, K. The unit of the K-value is  $m^2/W$ . As shown in the graphs the flame-spread velocity, becomes too fast.

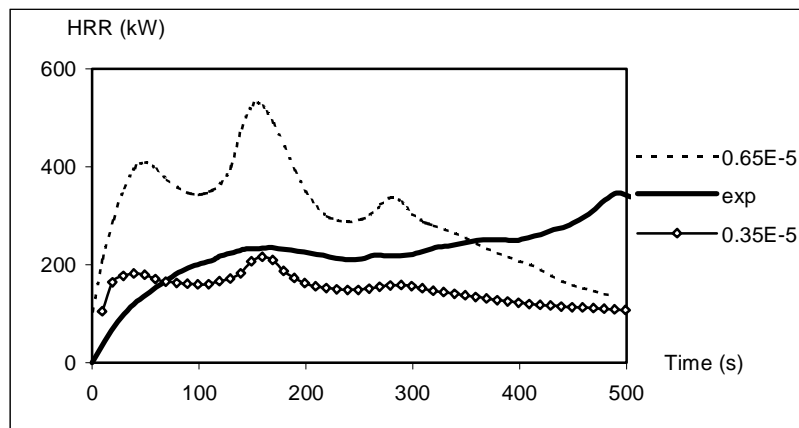


Figure G1. Porous fibre board on mineral wool

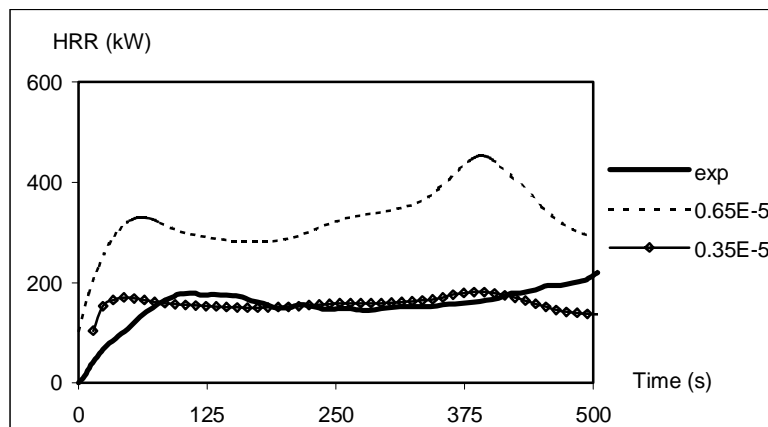


Figure G2. Wood (dry)

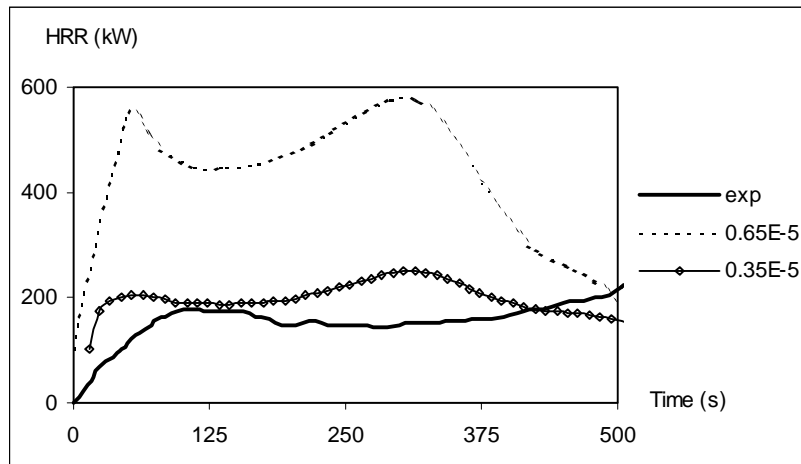


Figure G3. Wood (moist)

## APPENDIX H. MODEL B

This appendix shows the results from the evaluation of Model B. The materials show reasonable agreement with the experimental results especially the wood based. The upper layer temperature is generally underestimated by the WPI/Fire Code.

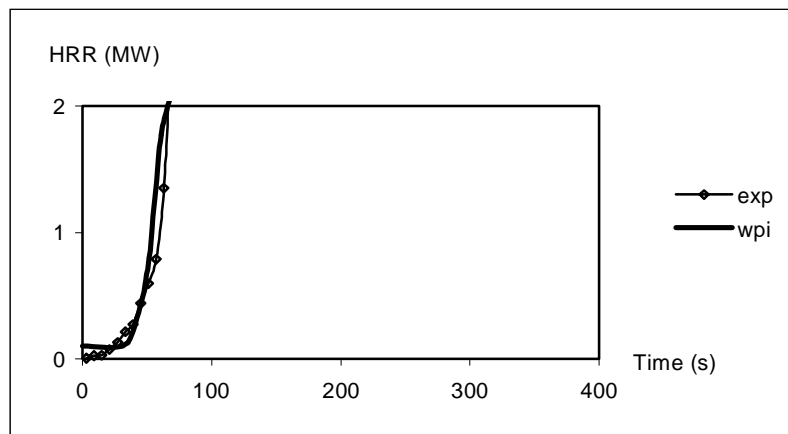


Figure H1. HRR of S1, insulating fiber board

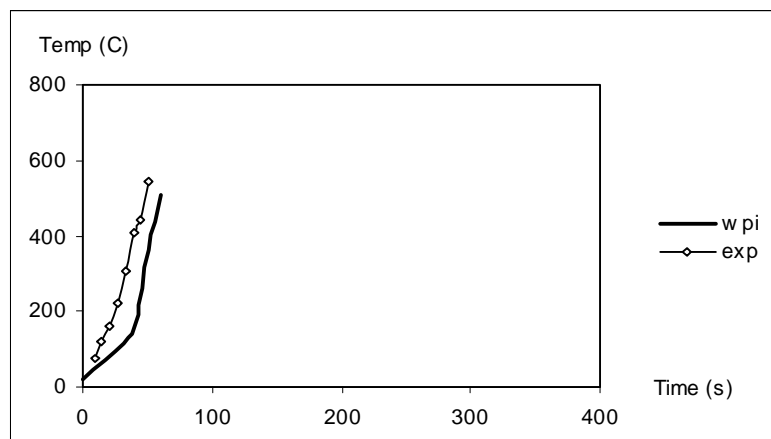


Figure H2. Upper layer temperature of S1, insulating fiber board

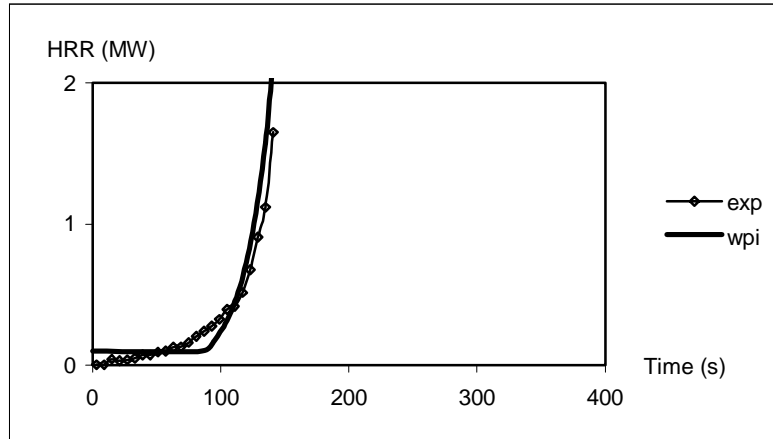


Figure H3. HRR of S2, medium density fiber board

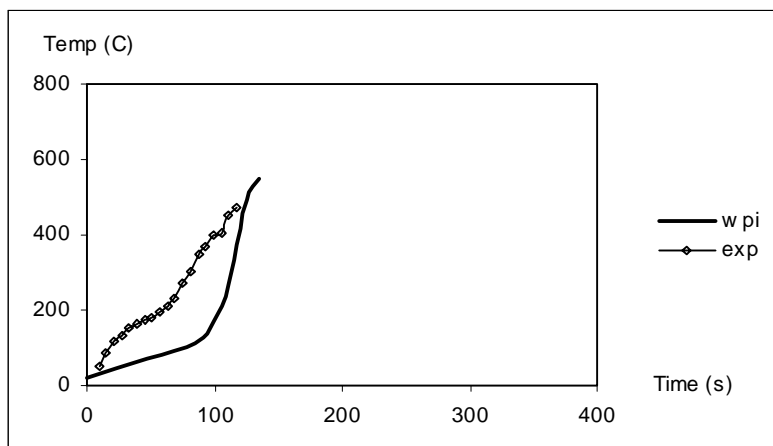


Figure H4. Upper layer temperature of S2, medium density fiber board

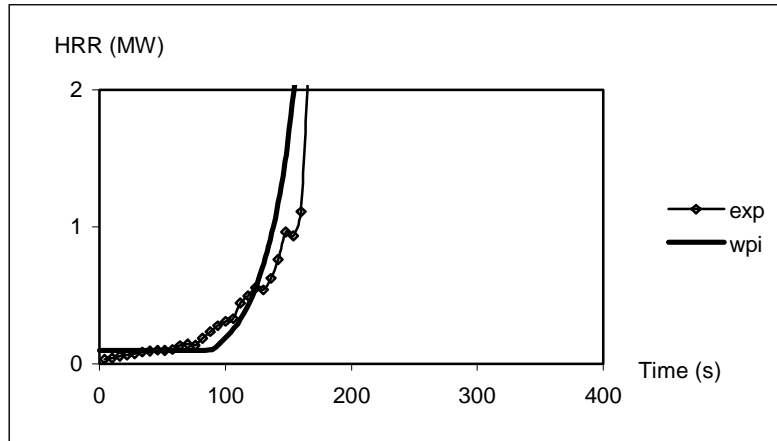


Figure H5. HRR of S3, particle board

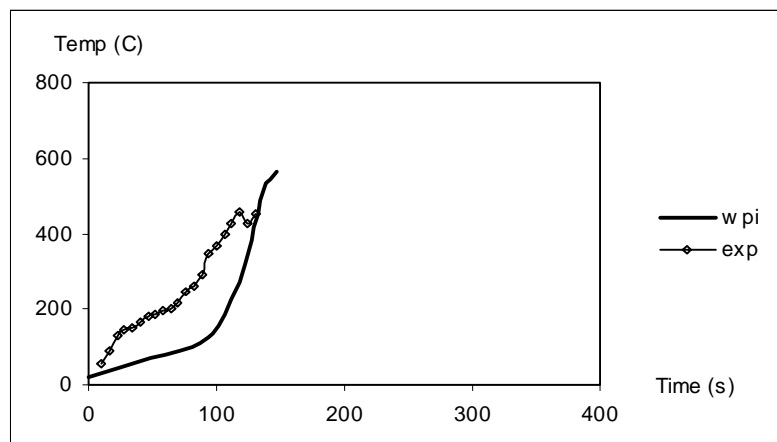


Figure H6. Upper layer temperature of S3, particle board

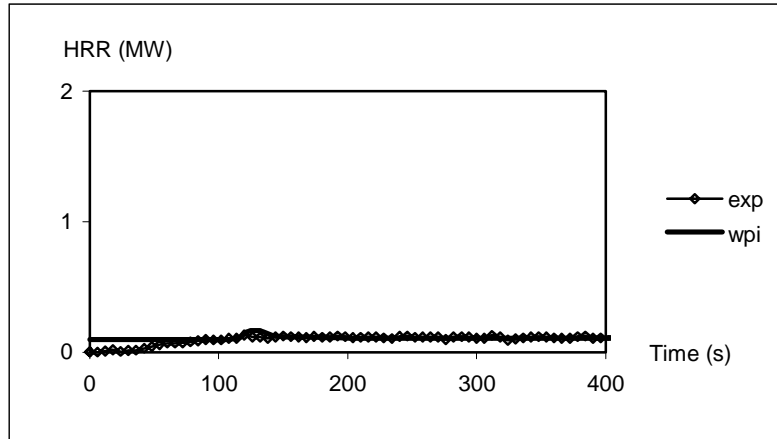


Figure H7. HRR of S4, gypsum board

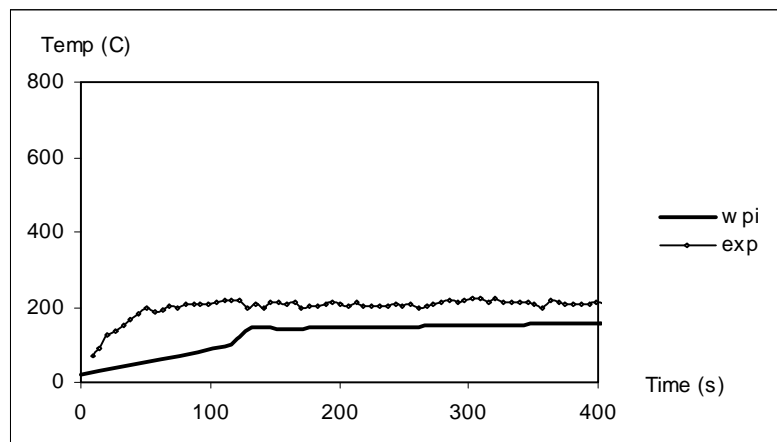


Figure H8. Upper layer temperature of S4, gypsum board

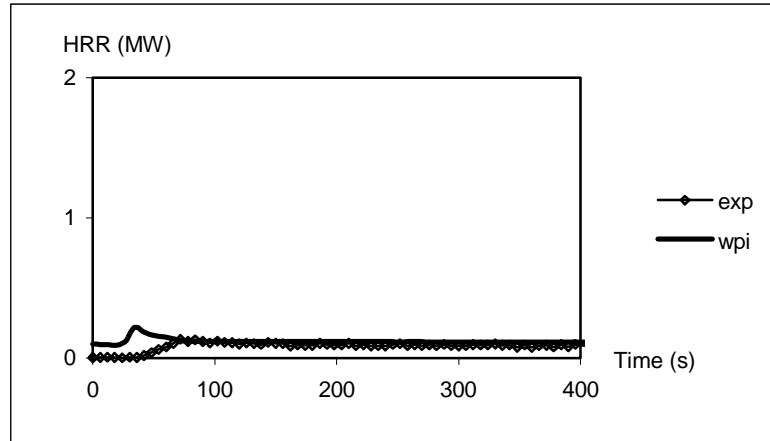


Figure H9. HRR of S5, plastic wall covering on gypsum board

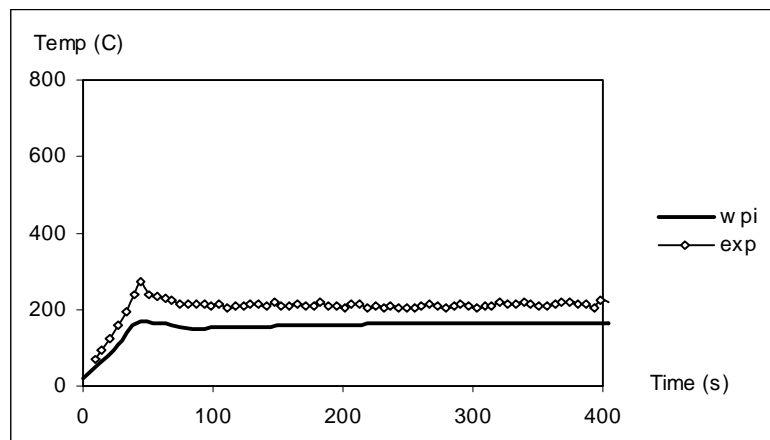


Figure H10. Upper layer temperature of S5, plastic wall covering on gypsum board

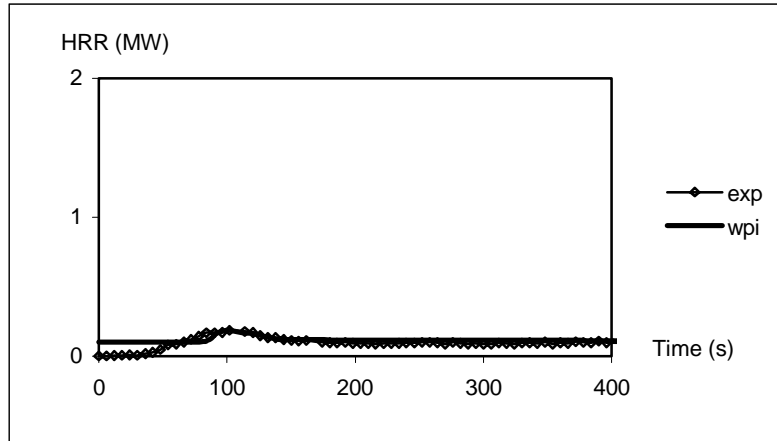


Figure H11. HRR of S6, paper wall covering on gypsum board

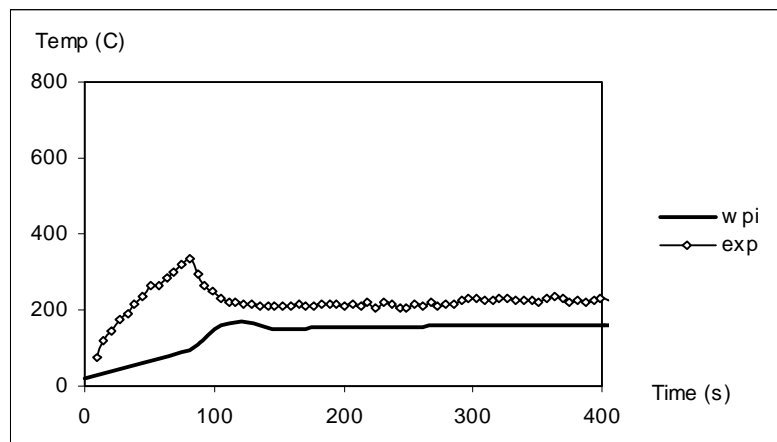


Figure H12. Upper layer temperature of S6, paper wall covering on gypsum board

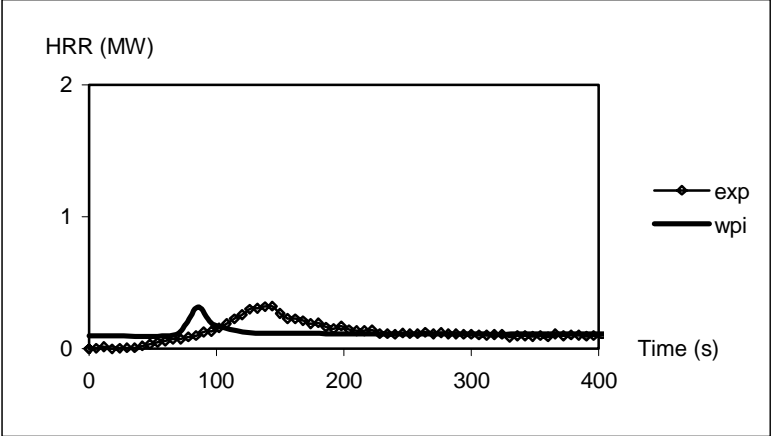


Figure H13. HRR of S7, textile wall covering on gypsum board

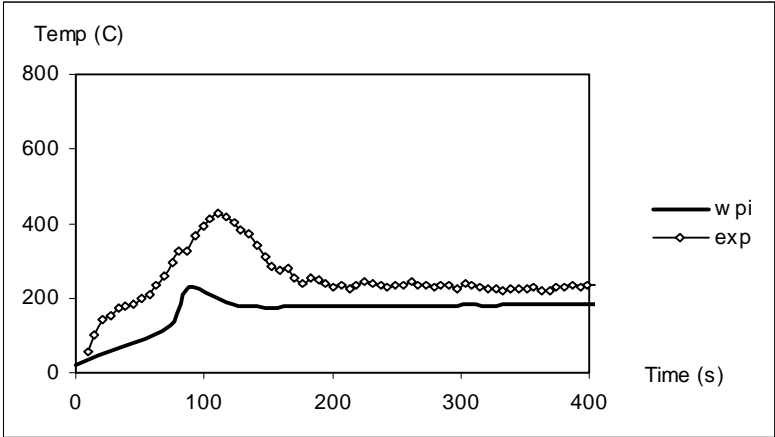


Figure H14. Upper layer temperature of S7, textile wall covering on gypsum board

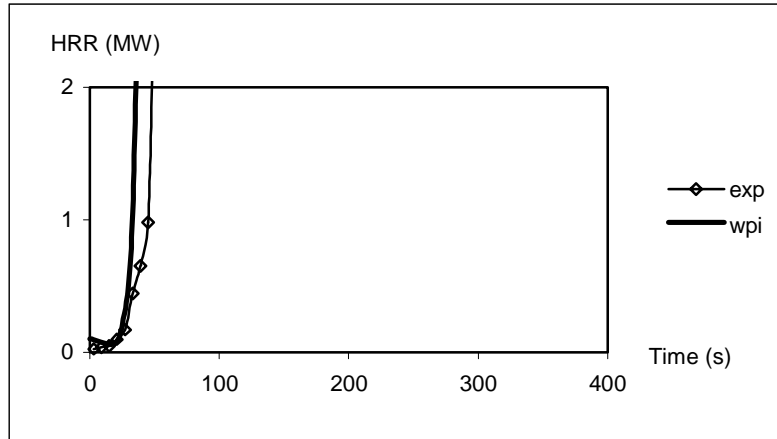


Figure H15. HRR of S8, textile wall covering on rock wool

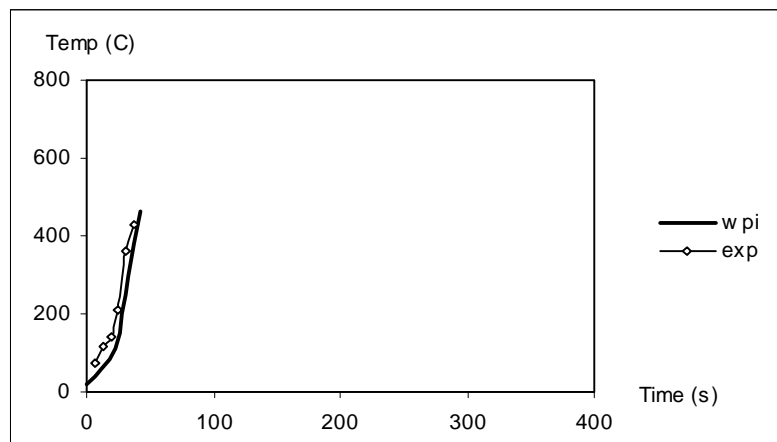


Figure H16. Upper layer temperature of S8, textile wall covering on rock wool

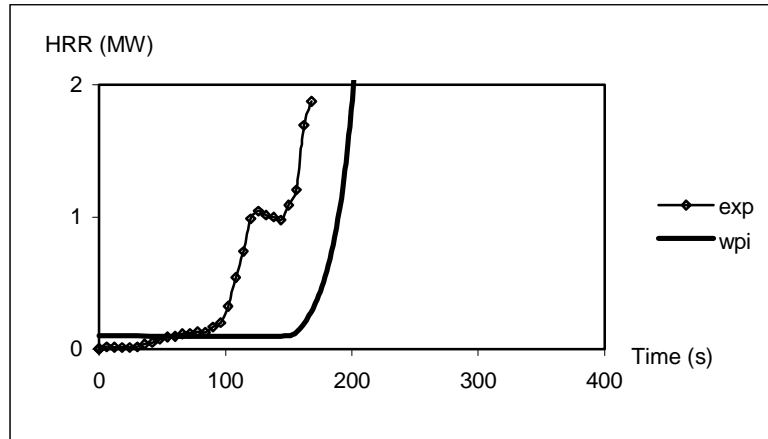


Figure H17. HRR of S10, expanded polystyrene

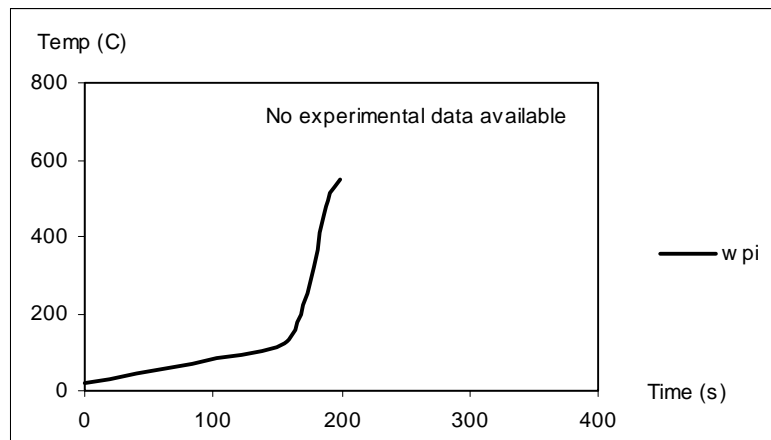


Figure H18. Upper layer temperature of S10, expanded polystyrene

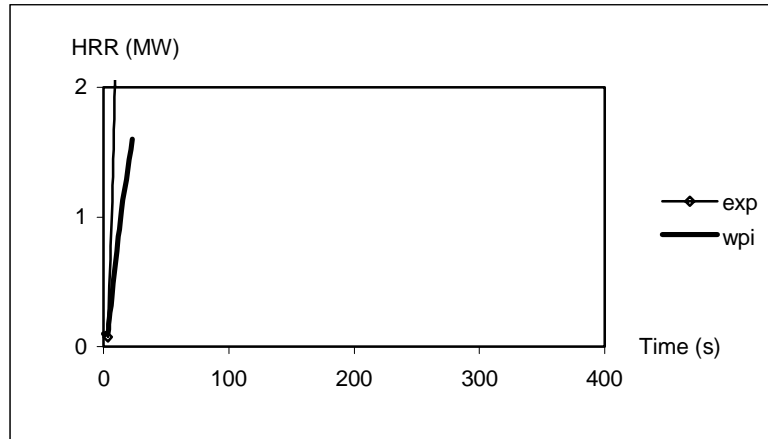


Figure H19. HRR of S11, rigid PUR

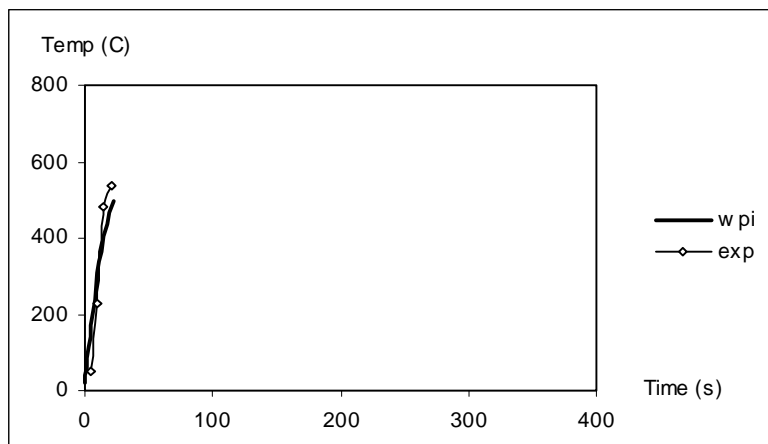


Figure H20. Upper layer temperature of S11, rigid PUR

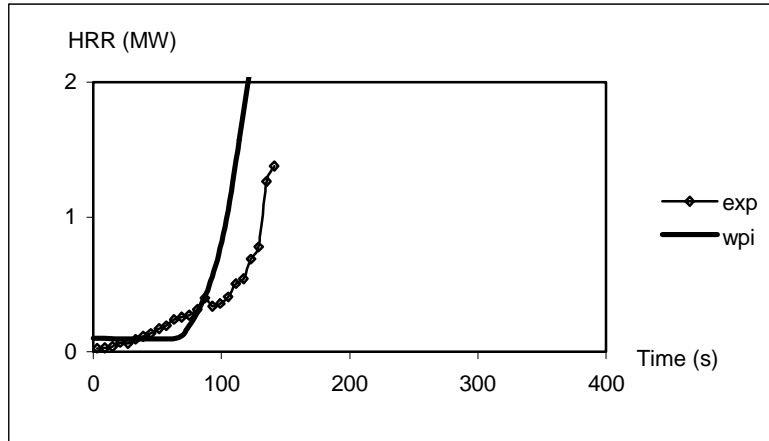


Figure H21. HRR of S12, wood panel (spruce)

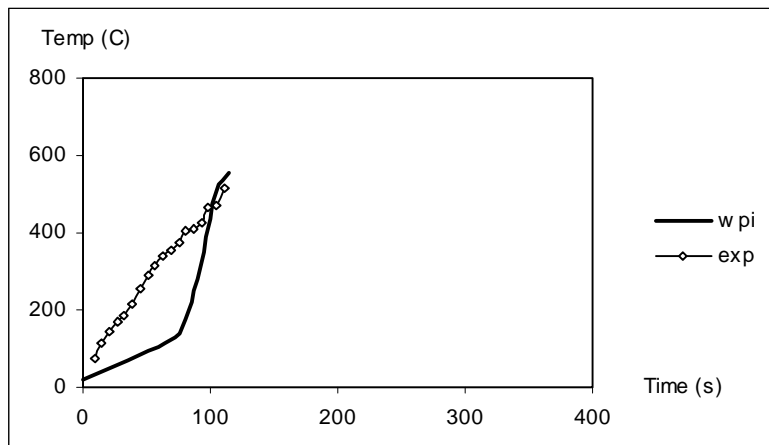


Figure H22. Upper layer temperature of S12, wood panel (spruce)

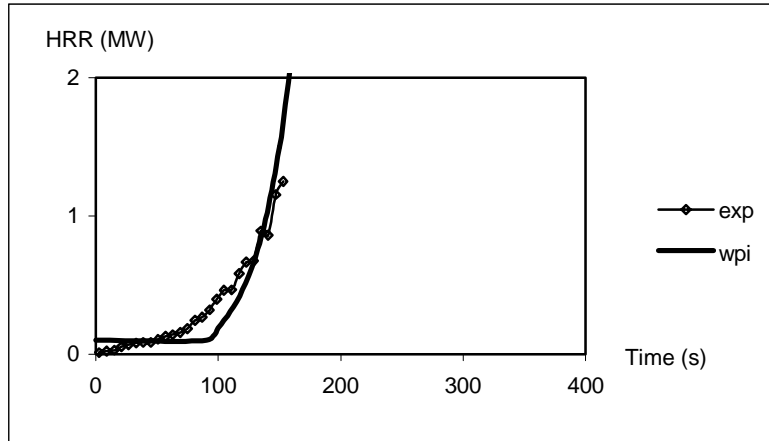


Figure H23. HRR of S13, paper wall covering on particle board

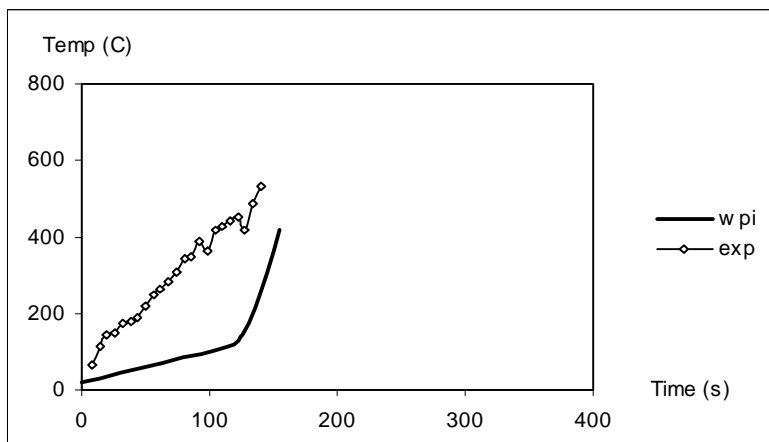


Figure H24. Upper layer temperature of S13, paper wall covering on particle board

**APPENDIX I. THE SOURCE CODE TO *THIMES***

This Appendix shows the source code to *Thimes*. Djebbar Baroudi programmed the original source code. However, several modifications have been made so it would be possible to integrate the code into the WPI/Fire Code.

```

C*****
C  THIMES.FOR : LAST MODIFICATIONS BY D. BAROUDI
C      21.01.1997
C      MODIFICATIONS:
C      =====
C
C*****
C  PROGRAMMED BY DJEBBAR Baroudi VTT/PAL
C  VTT (CENTRE OF SCIENTIFIQUE RESEARCH OF FINLAND) / FIRE TECHNOLOGY
C  =====
C
C  E-MAIL: Djebbar.Baroudi@vtt.fi (All comments are wellcomed)
C
C*****
C  Upward flame spread .... mallin ratkaisija
C  =====
C  OBS! KOKONAISTEHON EI SAA MENNÄ POLTIMEN JA PALNNEEN ALUEEN
C  TEHON ALLE
C
C  BACKWARD-EULER ! to be used ONLY
C      when q_cone_RHR(0) = 0 and      :==> A-Stable
C
C  FORWARD -EULER to be used EVERYWHERE
C      when q_cone_RHR(0) not equal to 0 :==> Stable if Dt<=2*tig
C
C*****

SUBROUTINE THIMES
IMPLICIT REAL*8 (A-H,O-Z)
PARAMETER (MNPROP=15)
PARAMETER (NVAR=2,MNPAR=1500)
REAL*8 TABLE(NVAR,MNPAR)
REAL*8 PROP(MNPROP)
C TILLAGG FOR NY TABELL DAR TID OCH MASSFORLUST SKALL LAGGAS IN!
REAL*8 ZASSA(2,1500)
COMMON /WRHR/ ZASSA
C
CALL DATDIM(NPROP,NPRINT)
CALL DATINP(NPROP,H,SA,SB,PROP,ZHObZZ,ZHWZM)
CALL RHRDAT(MNPAR,NPAR,NVAR,TABLE)

```

```

CALL INTDIF(NPROP,NPRINT,MNPAR,NPAR,NVAR,H,SA,SB,ZHObZZ,
&      ZHWZM, PROP, TABLE, ZASSA)
CALL CLOSFL

END

C*****
C  LIT LES DONEES D'ENTREE ET OUVRE LES FILES DE TRAVAIL  *
C*****
SUBROUTINE DATDIM(NPROP,NPRINT)
INTEGER NDIM,NPROP
CHARACTER*16 INFIL,OUFIL

C  WRITE(6,31)
C  WRITE(6,32)
C  WRITE(6,30)
C  WRITE(6,31)
C  WRITE(6,33)
C  WRITE(6,34)
C  WRITE(6,35)
WRITE(6,3)
READ(5,2) INFIL
WRITE(6,4)
READ(5,2) OUFIL
OPEN(UNIT=1,FILE=INFIL,STATUS='OLD')
OPEN(UNIT=2,FILE=OUFIL)
READ(1,*) NDIM,NPROP,NPRINT
c  WRITE(2,20) NDIM,NPROP
3 FORMAT(' NAME ON THE INPUT FILE TO WALL FIRE ? ')
4 FORMAT(' NAME ON THE OUTPUT FILE FROM WALL FIRE ? ')
2 FORMAT(A)
c 20 FORMAT(' NDIM =,I5,' NPROP =,I5)

C 31 FORMAT(' *****')
C 32 FORMAT(' ***** THIMES ***** by D. Baroudi***')
C 30 FORMAT(' ***** VTT / Fire Technology *****')
C 33 FORMAT(' **Modified by D.Gojkovic and H.Hultquist 1998* ')
C 34 FORMAT('*****')
C 35 FORMAT(' ')

RETURN
END

C*****
C  REMLIE LES TABLES A(NDIM) ET B(NDIM) *
C  H =ds :=dx :PAS DE L'INTEGRATION *
C  Sa = s1 , Sb = s2 ; (s1,s2):=INTERVAL D'INTEGRATION *
```

```

C  ZHObZZ(NDIM):=CONDITIONS INITIALES *
C*****
SUBROUTINE DATINP(NPROP,H,SA,SB,PROP,ZHObZZ,ZHWZM)
IMPLICIT REAL*8 (A-H,O-Z)
REAL*8 PROP(NPROP)

READ(1,*) (PROP(IPROP),IPROP=1,NPROP)
c  WRITE(2,200) (PROP(IPROP),IPROP=1,NPROP)

READ(1,*) H,SA,SB
c  WRITE(2,110) H,SA,SB
C    ZHWZM IS THE MAX. HEIGHT OF THE PANEL
READ(1,*) ZHObZZ,ZHWZM

c  WRITE(2,150)
c 110 FORMAT(' H =',E16.6,'SA =',E16.6,' SB =',E16.6)
c 120 FORMAT(' ALKUEHDOT=?')
c 200 FORMAT(' EPROP : ',10E12.6)
c 130 FORMAT(10E18.8)
c 140 FORMAT(' ALKUEHDOT')
c 150 FORMAT(' RESULTS')

RETURN
END

C*****
C  INTEGRATION PROPONENT DITE DU SYSTEME D'EQUATIONS *
C  DIFFERENTIELLE PAR LA METHODE DE EULER(EXPLICITE) *
C*****
SUBROUTINE INTDIF(NPROP,NPRINT,MNPAR,NPAR,NVAR,H,SA,SB,ZHObZZ,
& ZHWZM,PROP,TABLE,ZASSA)
IMPLICIT REAL*8 (A-H,O-Z)
PARAMETER (MNP=50000)
LOGICAL FPRINT
REAL*8 XFP(MNP)
REAL*8 PROP(NPROP)
REAL*8 TABLE(NVAR,MNPAR)
C TILLAG FOR TABELL MED TID OCH MASSFORLUST!
REAL*8 ZASSA(2,1500)
C  COMMON /WRHR/ ZASSA
C
MNIT=(SB-SA)/H+1
c  IF (MNP.LT.MNIT) THEN
c  WRITE(2,500)
c  WRITE(6,500)
c  STOP
c  END IF

```

```

I=0
S=SA
ZHBZZ=ZHObZZ
II=1

c  WRITE(2,300)
c  WRITE(2,201) S,ZHBZZ

10 CONTINUE
   I=I+1
   S=S+H

   CALL BEULER(MNPAR,NPAR,NVAR,MNP,II,NPROP,H,S,SA,SB,ZBObZZ,
&      ZHBZZ,ZHObZZ,ZHWZM,PROP,WEObZZ,WEOwZZ,WEOwbZS,ZHFZZ,
&      TLOwZZ,XFP,TABLE,TEOwbZS,TMOwbZS,TMObZZ,TMOwZZ)
C
C LAGGER IN TID OCH MASSFORLUST I EN TABELL (ZASSA).
   ZASSA(1,1) = 0
   ZASSA(2,1) = 0
   ZASSA(1,I+1) = S
   ZASSA(2,I+1) = TMOwbZS
C
C   FPRINT=(MOD(I,NPRINT).EQ.0)
C   IF (FPRINT) THEN
      WRITE(2,100) ZASSA (1,I),ZASSA(2,I)
C   TAR BORT DET SOM SKRIVS PA SKARMEN                               WRITE(6,200)
S,ZHBZZ,TEOwbZS,ZHFZZ,TLOwZZ
C SKRIVER UT TABELLEN ZASSA PA SKARMEN
C..  WRITE(6,*) ZASSA(1,I), ZASSA(2,I)
C   END IF
      IF (S.GT.SB) GOTO 20
      GOTO 10

100 FORMAT(F5.0, 9E14.6)
C 200 FORMAT('Time ZHBZZ TEOwbZS ZHFZZ TLOwZZ = ',5E10.3)
c 201 FORMAT(F5.0,E14.6)
c 300 FORMAT(' Time',T12,' ZHBZZ',T23,' WEObZZ',T34,' WEOwZZ',T45,
c   &      ' TEOwbZS',T56,' ZHFZZ',T67,' TLOwZZ',' TMOwbZS')
c 500 FORMAT(' Max.dim. XFP-table exceed. change MNP IN INTDIF.')
20 CONTINUE

RETURN
END

```

```

C*****
C  SYSTEME D'EQUATIONS DIF. A INTEGRER          *
C
C  TABLE EPROP(NPROP) CONTIENT DES PARAMETERS PASSES PAR
C  LE PROGRAMME PRINCIPAL. CES PARAMETRES SONT LUS DANS LA
C  ROTINE DATINP(...,EPROP) ET ENTRENT (OU PEUVENT ENTRER) DANS
C  LES EXPRESSIONS DES FONCTIONS A INTEGRER.
C
C  ALFA = 0 ==> BACKWARD EULER :==> A-STABLE
C  ALFA = 1 ==> FORWARD EULER  :==> C-STABLE, STABLE IF Dt <= 2*ZTIG
C*****
SUBROUTINE BEULER(MNPAR,NPAR,NVAR,MNP,II,NPROP,H,S,SA,SB,ZBObZZ,
&
      ZHBZZ,ZHObZZ,ZHWZM,PROP,WEObZZ,WEOwZZ,WEOwbZS,ZHFZZ,
&
      TLOWZZ,XFP,TABLE,TEOwbZS,TMOwbZS,TMObZZ,TMOwZZ)
IMPLICIT REAL*8 (A-H,O-Z)
INTEGER ALFA
REAL*8 XFP(MNP)
REAL*8 PROP(NPROP)
REAL*8 TABLE(NVAR,MNPAR)
REAL*8 N,KK
SAVE K

N =PROP(1)
X0 =PROP(2)
ZHBZI=PROP(3)
KK =PROP(4)
ZTIG=PROP(5)
T0 =PROP(6)
ZBObZZ =PROP(7)
WEObZM=PROP(8)
ALFA =INT(PROP(9))
FEOwZI=PROP(10)
QFw=PROP(11)
QFb=PROP(12)
CHI=PROP(13)

II=II+1

CALL CALCFT(MNPAR,NPAR,NVAR,TABLE,S,QRHR0)

C...  CALCUL DE Qflame=QFL0+QFL1
C...
      K=II

```

```
XPO=ZHBZI-X0
ZHFZI=KK*((WEObZM+FEOwZI*XPO)**N)
XFP(1)=(ZHFZI-ZHBZI)/ZTIG
```

```
IF (ALFA.EQ.0) THEN
  TJ=S
ELSE IF (ALFA.EQ.1) THEN
  TJ=S-H
END IF
TAU=T0
```

```
CALL CALCFT(MNPAR,NPAR,NVAR,TABLE,TJ-TAU,FEOwZZ)
QFL1=XFP(1)*H/2.*FEOwZZ
```

c QFLOT=QFL1

```
DO J=2,K-1
  TAU=T0+(J-1)*H
  CALL CALCFT(MNPAR,NPAR,NVAR,TABLE,TJ-TAU,FEOwZZ)
  IF (ALFA.EQ.0) THEN
    QFL1=QFL1+XFP(J)*H*FEOwZZ
  ELSE IF ((ALFA.EQ.1).AND.(J.NE.K-1)) THEN
    QFL1=QFL1+XFP(J)*H*FEOwZZ
  ELSE IF ((ALFA.EQ.1).AND.(J.EQ.K-1)) THEN
    QFL1=QFL1+XFP(J)*H/2.*FEOwZZ
  END IF
END DO
```

C...

C...

C.. XPO=ZHBZI-X0 määritelty aikaisemmin

C.. Calculates the RHR per unit width for the wall and the burner and the sum of them

```
QFL0=XPO*QRHR0
WEObZZ=WEObZM
WEOwZZ=QFL0+QFL1
WEOwbZS=WEOwZZ+WEObZZ
```

C.. Calculates the RHR for the wall and the burner and the sum of them

```
TEOwZZ=WEOwZZ*ZBObZZ
```

c.. TEObZZ=WEObZZ\*ZBObZZ

```
TEOwbZS=TEOwZZ
```

C.. Calculates the mass loss rate from the wall and the burner and summarize them

```
TMOwZZ=TEOwZZ/QFw/CHI
```

c.. TMObZZ=TEObZZ/QFb/CHI

```
TMOwbZS=-TMOwZZ
```

C.... SYSTEME A INTEGRER

```

C... PAR EULER BACKWARD :==> A-STABLE SCHEME IF ALFA = 0
C... PAR EULER FORWARD :==> C-STABLE SCHEME IF ALFA = 1 (STABLE IF
Dt<=2*ZTIG
C...
  ZHFZZ=KK*(WEOwbZS**N)
  IF (ALFA.EQ.0) THEN
    FT=(1./(1.+H/ZTIG))
    XPT=FT*(ZHBZZ+ZHFZZ*H/ZTIG)
  ELSE IF (ALFA.EQ.1) THEN
    FT=1.-H/ZTIG
    XPT=FT*ZHBZZ+ZHFZZ*H/ZTIG
  END IF

C**** BEGIN OF RECESSION OF THE BURNING FRONT
C.....
C... this takes the recession of the burning front into account AS COMMENTED BY B.
PARKER
C... SUGGESTED BY Parker Bill: IF xf(ti+1) < xp(ti+1) then set xp(ti+1)=xf(ti+1): kts.
Parkerin kommentit
C... ==> WEOwbZS >= Q_burner
C....FAIT LE 15.12.1996.....
C...
  IF (ZHFZZ.LT.XPT) XPT=ZHFZZ
C...
C**** END OF RECESSION OF THE BURNING FRONT

C*****
C Max. panel height limit suggested by V. Babrauskas
  IF (XPT.GT.ZHWZM) XPT=ZHWZM
C*****

  ZHBZZ=XPT
  TLOWZZ=(ZHFZZ-XPT)/ZTIG

C**** BEGIN OF PANEL HEIGHT EFFECTS: (SUGGESTED BY B. BABRAUSKAS)
C*****
C TLOWZZ=0 IS ADDED DY Djebar Baroudi, 14.6.1996
C THE MODEL : A)- CLASSICAL UPWARD MODEL FOR xp < Ymax, SEE D. Baroudi
C B)- IF Xp > Ymax ==> dxp/dt=0 :
C IF (XPT >= ZHWZM ) THEN TLOWZZ=0 (=dxp/dt)
C
  IF (XPT.GE.ZHWZM) TLOWZZ=0.
C
C**** END OF PANEL HEIGHT EFFECTS:

```

C... SAVES ZHFZZ-XP ---> TABLE XFP(I)

C...

XFP(II)=TLOWZZ

RETURN

END

SUBROUTINE CLOSFL

CLOSE(1)

CLOSE(2)

RETURN

END

SUBROUTINE RHRDAT(MNPAR,NPAR,NVAR,TABLE)

IMPLICIT REAL\*8 (A-H,O-Z)

CHARACTER\*72 RHRTXT

REAL\*8 TABLE(NVAR,MNPAR)

READ(1,1) RHRTXT

c WRITE(2,1) RHRTXT

IP=0

c WRITE(2,400)

10 CONTINUE

IP=IP+1

READ(1,\*,END=100) (TABLE(IVAR,IP),IVAR=1,NVAR)

c WRITE(2,300) (TABLE(IVAR,IP),IVAR=1,NVAR)

GOTO 10

100 CONTINUE

NPAR=IP-1

1 FORMAT(A)

c 300 FORMAT(2E14.6)

c 400 FORMAT(' Cone\_rhr : time q ')

RETURN

END

```
SUBROUTINE CALCFT(MNPAR,NPAR,NVAR,TABLE,T,FT)
IMPLICIT REAL*8 (A-H,O-Z)
REAL*8 TABLE(NVAR,MNPAR)

NDOM=MNPAR-1
DO 10 IDOM=1,NDOM
  IF((T.GE.TABLE(1,IDOM)).AND.(T.LT.TABLE(1,IDOM+1))) K=IDOM
10 CONTINUE

  I=K
  J=I+1
  DFTIJ=(TABLE(2,J)-TABLE(2,I))/(TABLE(1,J)-TABLE(1,I))
  FT=DFTIJ*(T-TABLE(1,I))+TABLE(2,I)

RETURN
END
```